THE DEVELOPMENT OF HEPARAN SULFATE WITHIN THE GLYCOCALYX

A Thesis by

Katelyn Reece

Bachelor of Science, Wichita State University, 2017

Submitted to the Department of Biomedical Engineering
and the faculty of the Graduate School of
Wichita State University
in partial fulfillment of
the requirements for the degree of
Master of Science

July 2020

THE DEVELOPMENT OF HEPARAN SULFATE WITHIN THE GLYCOCALYX

THE DEVELOPMENT OF HEPARAN SULFATE WITHIN THE GLYCOCALYX

The following faculty members have examined the final copy of this thesis for form and content and recommend that it be accepted in partial fulfillment of the requirement for the degree of Master of Science, with a major in Biomedical Engineering.

David Long, Committee Chair

Yongkuk Lee, Committee Member

Gary Brooking, Committee Member

DEDICATION

To my children.

ACKNOWLEGEMENTS

I would like to express my sincere gratitude to my advisor, David Long, for his guidance and support. This dissertation would not have been possible without his advice, patience and encouragement. I want to extend my gratitude to members of my committee Dr. Gary Brooking and Dr. Yongkuk Lee for their time and for serving as my thesis committee members.

I want to give a special thanks my lab members for their assistance in my experiments. Thank you to my family for being supportive and encouraging me to pursue further education.

ABSTRACT

A key to protecting vessel health occurs at the interface between circulating blood and endothelial cells. Strategically located at this interface is the endothelial glycocalyx, the first “line of protection” for blood vessels. The glycocalyx is a thin carbohydrate-rich layer of macromolecules that contain a variety of proteoglycans and glycosaminoglycans (GAGs). The glycocalyx is not only protective but is involved in a range of biological processes from nitric oxide production to cell-cell communication. While modulating numerous biological processes, the spatial and temporal distribution and composition of the glycocalyx can vary between a healthy and diseased state.

Since cultured endothelial cells may not display the same glycocalyx as the *in vivo*, the aim of this work was to confirm the presence of the most prevalent GAG, heparan sulfate, and image the development of heparan sulfate expressed on human microvascular cells type 1. This cell type was selected specifically for this project in that it can give a better understanding as to how this structure reacts to cardiovascular disease conditions. Heparan sulfate was successfully confirmed and proven to encompass the human microvascular cell type 1 over the course of time from three days post seeding to seven and a half days post seeding. Heparan sulfate was shown to be present by enzymatic degradation. Microscopy results show that the glycocalyx has the potential of being a surrogate and therapeutic marker for CVD as it does degrade when exposed to fluid shear stress which exhibits similar conditions to that of cardiovascular disease.. Future work can involve exposing this cell line to a fluid shear stress and imaging the degradation pattern of the glycocalyx. Successful completion of these experiments could encourage efforts to a possible therapeutic solution.

TABLE OF CONTENTS

TABLE OF CONTENTS (continued)

LIST OF FIGURES

LIST OF FIGURES (continued)

Figure Page

LIST OF ABBREVIATIONS

CVD	Cardiovascular Disease
CS	Chondroitin Sulfate
C_H	Concentration (High)
C_L	Concentration (Low)
DPBS	Dulbecco's Phosphate-Buffered Saline
EGCX	Endothelial Glycocalyx
ecSOD	Extracellular Superoxide Dismutase
GCX	Glycocalyx
GAG	Glycosaminoglycan
HS	Heparan Sulfate
HMEC-1	Human Microvascular Endothelial Cells
HA	Hyaluronic acid
HUVEC	Human Umbilical Vein Endothelial Cells
PBS	Phosphate Buffered Saline
ROS	Reactive Oxygen Species

CHAPTER 1: INTRODUCTION

1.1 Cardiovascular Disease

Heart disease, otherwise known as cardiovascular disease (CVD), is commonly associated with damage to the circulatory system. It is a chronic illness that is not caused by one variable but by a series of complex interactions such as inflammation, genetics, and leukocyte recruitment within the vascular vessels [1, 2]. *Cardiovascular disease* is an umbrella term for many different pathologies such as coronary artery disease, congenital heart disease, and atherosclerosis. Lifestyle choices can put individuals at an increased risk of developing CVD [4]. Conventional noninvasive methods that can assist in the treatment and prevention of CVD include increasing physical activity, eating a low-cholesterol diet, and ceasing smoking [5]. This disease is currently the leading cause of non-accidental deaths in the United State and is expected to grow two-fold by the year 2030 [3]. Given this expectation, it is imperative that the healthcare industry and human population are proactive in the prevention, early diagnosis, and early treatment of this disease.

Atherosclerosis is the principal factor that underlies the progression of CVD [1]. It is primarily associated with the build-up of atherosclerotic plaque within the coronary or carotid arterial wall, which over time, can cause a complete disruption of blood flow. This disruption can eventually lead to a stroke or myocardial infarction. The plaque build-up consisting of leukocytes, cholesterol, and other cellular constituents are attracted to inflammation and signs of injury within the vascular wall.

When inflammation occurs within the vascular wall, leukocytes respond and adhere to the endothelium [1]. This plaque build-up can damage the artery over time while hardening and narrowing the artery, thereby impeding blood flow to the rest of the body. These sites tend to be areas where disturbed blood flow occurs. This disturbed flow affects the hemodynamic force experienced by the cells lining the blood vessels (endothelial cells). Previous experimental studies have shown that blood flow can alter endothelial cell morphology and endothelial gene expression [2-4]. Moreover, disturbed flow can activate endothelial cells to initiate cardiovascular disease. In time this build-up can rupture. This process is visually demonstrated in Figure 1.1 [1]. Figure 1.1 A shows the vascular wall which allows the white blood cells to enter the tissue. Figure 1.1 B represents the recruitment phase wherein more leukocytes travel to the site. Figure 1.1 C showcases a plaque rupture [1]. This event elicits a response from platelets, which are known as the first line of defense following injury. During the interaction of platelets and leukocytes, platelets mistake this rupture as vascular bleeding and begin to form a clot, a process known as thrombosis, to fix the perceived damage [2].

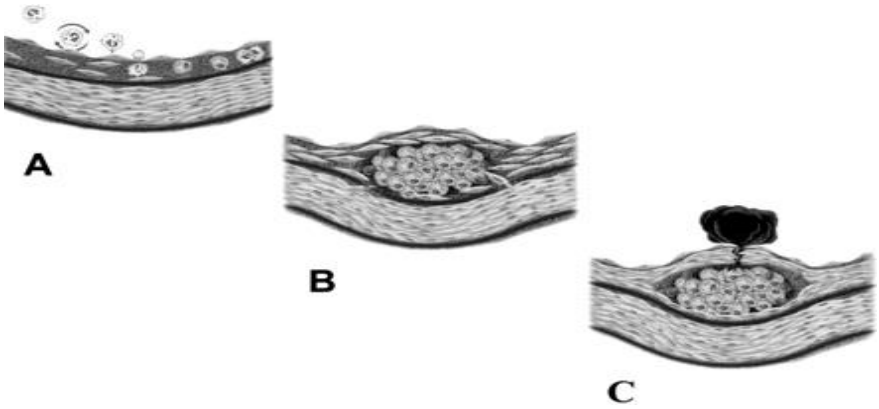

Figure 1.1 Leukocyte recruitment and rupture [5].

A: Luekocyte recruitment to atherosclerotic lesion. B: Lymphocytes enter the intima region during lesion evolution. C: The fibrous cap that protects the blood from plaque begins to weaken and rupture. Once ruptured a thrombus forms that is responsible for complications of atherosclerosis.

Figure 1.2 the process from the perspective of blood flow. The cartoon illustrations demonstrate the process in which over time the blood flow becomes obstructed and eventually ceases, thereby causing a blockage [3]. When there is an obstruction within the vascular wall, turbulent flow will occur. Turbulent flow is described as “chaotic” and can occur in curvatures of arterial branch points as well as in diseased arteries. Turbulence increases the energy needed to generate blood flow. This behavior would typically promote tissue healing in situations which involve inflammation. However, in this case the risk of platelet aggregation increases while also accelerating the progression of atherosclerosis [4].

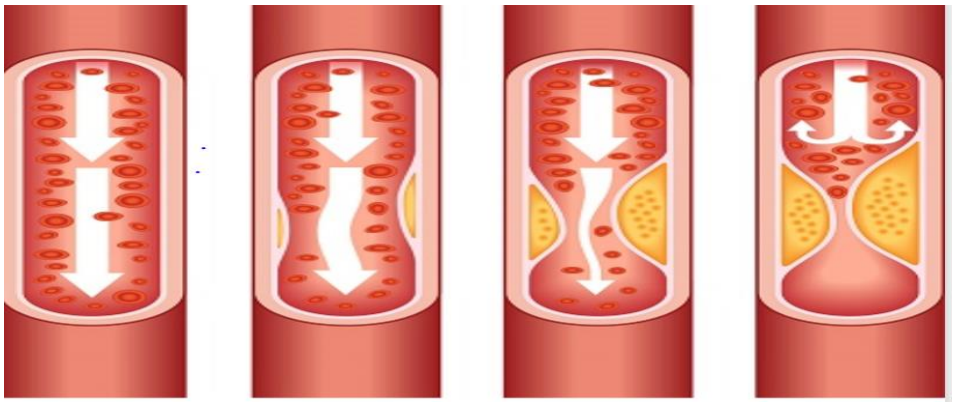

Figure 1.2 Representation of blocked blood flow within artery due to plaque buildup [6].

1.2 The Glycocalyx

The glycocalyx (GCX) is a carbohydrate-rich thin layer that is expressed on the apical membrane of cells that line the vascular network [7]. The composition of the GCX contains glycoproteins and glycans, including heparan sulfate (HS), the most prevalent glycosaminoglycan (GAG). A model of the GCX is represented in Figure 1.3 and Figure 1.4. Heparan sulfate is a diverse GAG that regulates many biological processes which are dependent on what cell type it lies within. The role of this sugar chain in CVD is discussed further in chapter 2.

Figure 1.3 Representation of blood vessel lined with endothelial cells. (orange) Endothelial cells. (green) Glycocalyx. (Red) Transmembrane protein [8].

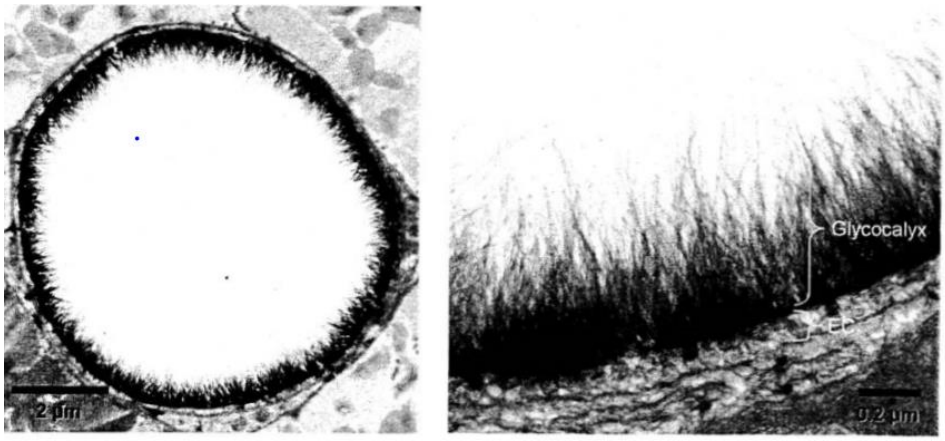

Figure 1.4: Electron micrograph of a goat coronary capillary stained with Alcian blue [9].

The GCX has been found to maintain homeostasis and to be involved in regulatory processes of mechano-transduction and vascular permeability [8]. The GCX is dynamic and can transition from a healthy state to a diseased state depending on the microenvironment of the cell. Because the GCX lies on the apical side of endothelial cells, it is in direct contact with fluid shear stress from the flowing blood. Given this structure's

location and endothelium function, it is promising that it can be a surrogate marker and therapeutic target for CVD [10].

1.3 Purpose of this study

The two goals for this current study are the following, (1), to determine that the cell line of interest, human microvascular endothelial cells Type 1 (HMEC-1), does contain the GAG, HS, and, (2), to evaluate how HS develops around the cell over time in culture. The rationale for these goals is the following: how cells modify and display their GCX during disease development, we need to monitor the dynamics on living cells.

This growth pattern can give us a greater understanding of how the GCX regenerates when it is degraded due to fluid shear stress or systematic risk factors such as hypercholesteremia. During this degradation process, many other properties likely falter, such as mechano-transduction regulation and hemo-dynamic processes [3]. When these problems occur, the cell's healthy state can become compromised. The current project was created as a small step towards a larger goal: to eventually understand the GCX with all major GAGs, as is discussed further in the following sections. The cell line studied in this thesis is unique to this field of research, as it has not been studied extensively in CVD. The standard endothelial cell lines that have been studied for this purpose are the following: (1) human umbilical vein endothelial cells, (2) animal lines such as bovine aortic endothelial cells, and, (3) rat-fat pad endothelial cells. Though these cell lines can give insight into the biological processes of the human body, due to the nature of their host they can be restrictive when demonstrating GCX behavior across all species and cell lines. Many different cell types may behave similarly in response to

fluid shear stress or other mechanical stimuli, but not all cell lines respond the same to stimuli. To clearly understand the body's response when it is exposed to disease, we need to expand on the types of cells studied. The HMEC-1 line from the microcirculatory system serves as a protective barrier to inflammation, pathogens, and disease [11]. These cells are resilient to disruption and are easy to maintain. There is a large amount of knowledge to gain regarding how HMEC-1 plays a role in CVD in respect to disturbed conditions such as degradation or shear stress [12, 13].

The research presented here will explain the background research (the importance of the GCX and the role of HS within the structure), the current study proving the existence of HS in HMEC-1, and how this knowledge is important for future research for treatment of CVD. It is necessary to prove the existence of the component, HS, as it has been shown in the past that the GCX may not be shown in its entire form on endothelial cells. Hence why it was chosen to study the GAG, HS, as it is the most prevalent GAG and the most likely constituent to be seen on the HMEC-1 cell line being studied. Chapter 2 includes past research completed on the GCX thickness, biological responsibilities, and its' core constituents. Chapter 3 discusses the preliminary studies completed in order to confirm that the positive control does correlate with the antibodies chosen. It outlines the development of the protocol and determinations the antibody dilutions used for future experiments. Chapter 4 includes the studies to confirm HS is expressed on HMEC-1 cells in culture and demonstrate the development of HS over a series of time. Chapter 5 outlines the enzymatic degradation of heparan sulfate in the HMEC-1. It includes the process of determining and testing different enzyme concentrations.

Chapter 6 summarizes the results from this research and provides recommendations for future work in this study.

CHAPTER 2: LITERATURE REVIEW

2.1 Overview

Within our blood and lymphatic vessels, a thin layer of endothelial cells lies facing in the direction of blood flow. These cells serve as an essential barrier between the exchange of fluid inside the vessel and the rest of the vessel wall. Endothelial cells have a thin layer of glycans covering their surface, which is known as the endothelial glycocalyx (EGCX). This complex is a carbohydrate-rich structure that protects the cell surface from negative interactions such as the breakdown of the vascular wall (due to fluctuating blood flow) and leukocyte adherence that propagates inflammation and could alter the structure's mechanisms that protect against disease. Imaging the GCX did not become popular until the late 1990s, when it was discovered that the GCX was involved in arteriole permeability and that disruption of it could cause physiological diseases such as diabetes, CVD, cancer, kidney disease, sepsis, and other fatal diseases [14-16]. The discovery started a recent boom in research targeting the GCX and how its properties affect the biological system. The GCX serves as a biological surrogate marker and is currently investigated as a therapeutic target.

2.2 Biochemical Structure of Glycocalyx

The carbohydrate-rich mesh known as the GCX is a thin endothelial surface layer that covers all vascular walls. This complex structure is responsible for regulating micro-vessel permeability and hemodynamics [17]; it is supplemented by various proteins: glycoproteins, proteoglycans, and GAGs [18]. The composition of this endothelial surface layer is dynamic and is continuously regenerated to replenish the continually shedding structure caused by disorder [7]. The biochemical structure is illustrated in Figure 2.1.

Glycoproteins are known as backbone molecules, as they connect the GCX to the endothelial cell membrane. These proteins are relatively small, with a few short carbohydrate side chains covalently attached by glycosidic bonds. These chains make up 50-60% of the total weight of the structure and can be positively or negatively charged. Glycoproteins are important to modulating cellular development processes [7].

A subclass of glycoproteins with polysaccharide side chains is known as proteoglycans [7]. They are found in all connective tissues and their size and density vary [19]. They include a protein core to which negatively charged GAGs chains attach [20]. These core protein groups are syndecans, glypicans, mimecan, perlecan, and biglycan.

Syndecans are anchored to the plasma membrane by hydrophobic domains, while glypicans are attached to the membrane by a GPI anchor [21]. The others mentioned are smaller proteoglycans with approximately one to two GAG side chains. They are secreted after the assembly of the GAG chains [22]. The purpose of the proteoglycan depends on what GAGs are attached.

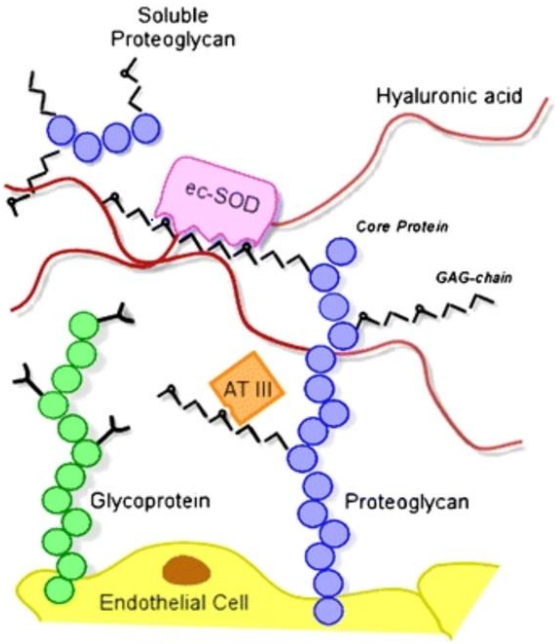

Figure 2.1 Schematic representation of glycocalyx and main components [7]

Glycosaminoglycans are chains which consist of hundreds to thousands of disaccharides bound to the transmembrane by the adhesion molecules known as syndecans [21]. There are five types of GAG chains: heparan sulfate (HS), chondroitin sulfate (CS), dermatan sulfate, keratan sulfate, and hyaluronic acid (HA). Of these; CS, HA, and HS are the three most abundant [7]. Heparan sulfate accounts for 50-90% of all GAGs, thus making it the most extensively studied [23, 24]. Compared to CS and HS, HA is a more extended disaccharide polymer and the only GAG that does not bind to a protein core [23]. It is assembled in the cytosolic side of the cell membrane and has no sulfate groups or modification patterns [7]. This GAG plays a vital role in mechano-transduction and glomerular filtration [25]. The HS and CS are produced in the endoplasmic reticulum and Golgi apparatus of the endothelial cell. It is there that a primary linker is added to start the GAG chain. After the addition of the primary linker, different galactose-residues are added to differentiate the various types of GAG chains [7, 26]. After chain polymerization, the chains undergo modifications while determining the final type and functionality of the proteoglycans to which they attach [7]. It has been shown that these modification patterns can vary under different pathophysiological conditions [27]. The CS and HA play a significant role in regulating permeability, as the diffusion rate increases after enzymatic degradation of these components [28]. They could be more prevalent on the surface of the glycocalyx, where more diffusion takes place. This could mean that they may need to be restored more frequently than other components that lie below the surface. Heparan sulfate is involved in mechanisms of cell adhesion, and proliferation

[29]. The GAGs- most notably endothelial-type nitric oxide synthase- are involved as a single unit in vesicular transport and cell signaling [23].

2.3 Physiological Function of Glycocalyx

The endothelium lines the inner cellular lining of the vascular system. It is very adaptable and participates in processes such as blood flow, permeability, and immune response [30]. The GCX forms the outer cortex of the endothelium and serves as the first line of defense against contact with blood [8]. When the endothelium cells are exposed to shear stress, they produce nitric oxide [7]. The GCX's function is to convert this biochemical force into a biochemical signal such as nitric oxide and to produce or reorganize the cytoskeleton [31]. For the mechano-transducer GCX to carry out this process, the core proteins of the structure and the attached GAGs must be in a healthy condition. Enzymatic treatment of GAGs has shown that the production of nitric oxide ceases, thus suggesting that the GCX has a direct effect on nitric oxide production [32]. Nitric-oxide release mediates flow-induced vasodilation, as nitric oxide tells the muscle cells around the blood vessels to contract or relax. To regulate blood flow, the changing diameter maintains homeostasis in the tissue [31]. Studies of the carotid artery of mice have shown that the GCX composition is shear-dependent due to a correlation between shear stress and the dimensions of the GCX. Laminar flow shows a thicker profile; disturbed flow is followed by a thinner GCX layer [33]. Disturbed blood flow is continuous with high blood pressure, which can put extra strain on the heart and vessels. This reaction can in turn cause a buildup in plaque. Over time, this increases one's risk of disease.

The entire surface of all vascular walls is covered with a mesh known as the GCX. This GCX dictates what interactions take place between the cells and components around it, such as blood and proteins [34]. It is in control of red and white blood-cell mechanics, signaling, and the transmission of shear forces [35]. It is permeable to molecules based on size and charge. It repels negatively charged molecules and does not allow the passage of molecules greater than 70 kilodaltons. Sialic acid residues that cap the ends of glycoproteins are the principle regulators of micro-vessel permeability [34]. Inflammation of the structure caused by proinflammatory cytokines can rupture the structure, thereby increasing permeability and making it susceptible to disease [36]. Thickness is associated with vascular permeability as the entry of invading organisms into the structure or increased blood flow could remove the core proteins, thus resulting in an unstable, thinning structure [37]. Therefore, the structure is thicker in un-diseased arteries than in those that are diseased and accumulate plaque. The thickness changes in response to changes in arterioles, capillaries, and venules [38]. Shedding of the GCX can occur in response to inflammation, abnormal blood-shear stress, hemorrhagic shock, and surgery. These mechanisms can activate adhesion molecules to attach to the endothelial cell surface, thereby increasing its resistance to flow [39]. This resistance is supported by research which shows that the apparent thickness of the GCX is greater than that of a cell with leukocyte rolling and adhesion [40]. If plasma proteins were absent, the GCX structure would collapse due to the elimination of intramolecular interactions [41].

2.4 Pathophysiological Function of Glycocalyx

The GCX serves as an identifier for the body to distinguish between healthy cells, diseased cells, or invading organisms [42]. If disruption to this structure were to occur, the disease would have a possible detrimental effect. This structure is involved in several diseases, including CVD, cancer, kidney disease, and sepsis. Albuminuria is an early marker for kidney disease. The protein albumin is present in the urine instead of being used as a nutrient to the body's tissues and muscles. Albumin binds tightly to the GCX even though it has a net negative charge. This binding reduces the hydraulic conductivity across the vascular barriers. This reduction can cause an albumin leak, which could then disrupt the GCX and lead to hyperpermeability. The enzymatic removal of the GCX can significantly aid the passage of albumin through the glomerular filtration barrier [14]. Albuminuria is a condition that commonly follows the swelling of kidneys and can be risk factor for diabetes and CVD [43].

The GCX provides protection against inflammation and vascular leakage in sepsis [22, 44]. Since GCX thickness does decrease in most diseases, stiffness corelates and decreases as well. When stiffness decreases, the resistance of the GCX to outside forces and pathogens decreases, thus leading to hyperpermeability. This is a sign that inflammation-induced damage has occurred. Angiopoiten-2 is a naturally occurring antagonist protein to the agonist ligand Angiopoietin-1. Angiopoiten-2 contributes to plasma leakage, which promotes infection [45]. Stiffness has been shown to be altered by high levels of lipopolysaccharides, thrombin, and nitric oxide production, which are common in sepsis. This infection gives patients an increased risk of CVD. Schmidt et al. recently announced that preventing degradation of heparan in the GCX would decrease

vascular hyperpermeability and leukocyte adhesion, thereby decreasing the risk of sepsis [15].

Frey et al. found when using ultrastructure examination that carcinoma enterocytes lacked a mature GCX on their membranes. This encouraged Ramaker to use electron microscopy to observe colorectal tissues by tagging receptors underneath the GCX and thereby show its absence [46]. Malignancy causes an altered expression in the glycans and glycoproteins that contribute to the surface of the GCX. These tumor-inducing changes increase the expression of large glycoproteins that promote integrin adhesion and affect receptor function by mediating interactions between signaling pathways. These large glycoproteins can foster tumor development and metastasis [47].

2.5 The Glycocalyx is a vital part in Cardiovascular Physiology

The EGCX is responsible for the regulation of vascular permeability and for providing a barrier to the cell surface by preventing contact between leukocytes and platelets that promote blood coagulation [48]. This thrombotic response is directly associated with human CVD. In CVD, shear stresses induced by the disturbed blood flow affect the dynamics of both the GCX and its molecular constituents. These shear distributions over the GCX are not uniformly distributed and influence the mechano-transduction process and pathophysiology [49]. The GCX sheds in response to atherosclerosis, taking away its job as the first line of defense against invading organisms and diseases. This degradation alters its cell:cell communication abilities while increasing its inflammatory response to inflammatory cells. These cascades of events reduce the

expression of nitric-oxide synthesis. Nitric oxide serves as a vasodilator and, without it, vasoconstriction can occur [50]. Current research involves creating a computational model of the GCX and its sugar chains and presenting it with changing dynamics of flow to observe the behavior. This could enhance our understanding of the GCX in diseases such as CVD [49].

2.6 Heparan Sulfate's role in Glycocalyx Structure Thickness

The GCX has served as an important regulator for mechano-transduction, and its thickness and ultrastructure determine this function. It has previously been discovered that these components shed in response to the cell transitioning to a diseased state [51, 52]. The GCX exhibits a natural shedding process due to hemodynamics that makes the structure dynamic. However, rapid shedding of the structure and its key components can alter its properties such that the structure adopts a disturbed phenotype. Exploring the behavior of GAGs and proteoglycans during this crucial time could contribute to understanding how they respond to their physiological environment. The most prevalent GAGs have been studied to determine their contribution to GCX function and thickness. The GCX has been measured by different microscopy techniques, and different thicknesses have been published, as these vary between the species of cell line studied [37, 50, 53]. One common outcome of research is that, when enzymatic degradation occurs targeting specific GAGs (CS, HA, and HS), the thickness of the whole structure diminishes by approximately 90%. This result suggests that these GAGs contribute most of the thickness of the glycocalyx. When HS is treated with the enzyme heparinase, the GCX decreases significantly by approximately 43% [37] [54]. With these results, it is

assumed that this GAG is the most prevalent. The varying results in the GCX thickness and diffusion coefficient, mentioned previously, suggest the possibility that these GAGs are not evenly distributed and that some may lie in the deeper layers while others lie on the surface, thereby supporting previous and future studies [28, 54]. Degradation of these GAGs and other components alter the integrity of the structure in more ways than permeability and thickness. The GCX components have also been found to be involved in nitric-oxide production, mechano-transduction, permeability, and hemodynamics [34, 39, 55, 56]

2.7 Heparan Sulfate's involvement in Nitric Oxide Production in Cardiovascular Disease

Nitric oxide is an important regulator in vascular tissue and arterial walls [50, 57]. It is responsible for vasorelaxation, inhibition of leukocyte adhesion, and protection from diseases such as atherosclerosis and diabetes. Nitric oxide increases in correlation to perfusion rate, which is an increase in blood flow. This explains why exercise is crucial in day-to-day life: it increases shear stress and nitric-oxide release, which decreases the risk of CVD. It is produced from friction between endothelial cells and fluid shear stress. In areas of disturbed blood flow, such as in the coronary arteries, there can also be areas of low shear stress. These areas can have a buildup of plaque such that less nitric oxide is being produced and vasoconstriction takes place. This narrows the arteries, thus making it harder for blood to flow through. If the flow was to stop or form a clot, a heart

attack or stroke could occur. Disturbed blood flow could also cause degradation of the EGCX that lines the walls of vessels and arteries, which in turn compromise the production of nitric oxide and oxygen [55].

Extracellular superoxide dismutase (ecSOD) lies within the GCX and serves as a "scavenger" of free radicals that lie in the vessel wall and regulates the bioactivity of nitric oxide. If disruption of ecSOD would occur, oxidative stress could be result leading to vascular diseases. Free radicals target proteins and damage cells, thus making the GCX a perfect target due to its protein rich structure [4]. Research has been done to show how the GCX and its components are implicated in nitric oxide activation and reactive oxygen species (ROS) synthesis. It was proven that after enzymatically degrading GAGs the diameter of vessels decreased, and wall shear stress increased. Constriction will take place leading to diminishing nitric oxide production. Superoxide production increased in correlation to the diminishing HS, the dominant GAG of the GCX [12, 55]. Treatment with the enzyme heparinase abolishes the nitric oxide response to elevated rates of shear stress in which endothelial cells are exposed to. With degradation of the this piece of the EGCX, EcSOD reduces leading to an elevation of ROS production and less regulation of nitric oxide[55]. With the reduction of HS correlating to the reduction in nitric oxide production, it can be determined that this GAG is a shear stress sensor. When disturbed shear stress occurs, the placement of this essential GAG shifts and adopts a new orientation, promoting a response within the cell. Though HS is most responsible for the GCX thickness, it is needed to be significantly removed for a significant negative effect on nitric oxide production to take place [12]. This is referred to the threshold level in which a point must be reached for an action to occur.

2.8 Therapeutic Options for GCX Dysfunction

Many diseases are associated with compromised GCX health, specifically, CVD [10, 48]. As one of the regulatory and protective properties, the GCX is responsible for filtration and restricts the passage of certain molecules. When compromised, the GCX increases its permeability. This creates the possibility that something of the nanoparticle scale could travel to the targeted region at this time with a form of treatment. Gold nanoparticles are currently being studied as a form of drug delivery through the blood stream to “hard to reach” locations. These nanoparticles can be coated with biological agents which depend on the selectivity of the tissue they are traveling to. More research needs to be done on this form of treatment to verify that it is in fact treating the diseased region and not becoming toxic over time. Successful treatment of the GCX with these nanoparticles could improve other drug delivery methods [58, 59].

It has been made apparent how the GCX is involved in arterial-wall thickness, vascular permeability, and nitric-oxide production [10, 32]. As mentioned previously, most research involving the GCX has been completed with the use of bovine aortic endothelial cells or human umbilical vein endothelial cells (HUVECs). It is assumed that not all cell types respond or behave the same, thus encouraging expansion of the cell types being studied regarding this structure. In this thesis, the goal is to study how the most abundant component of the human GCX, the HS, develops over time within HMEC-1. This chapter reviewed past research on the biological functions of the GCX in healthy cells as well as diseased. Then it was discussed how HS (and other less prevalent GAGs) plays a role in those biological functions for example nitric-oxide production and mechano-transduction

regulation. One of the specific aims of this work is to open the potential for future research on the specific cell line, HMEC-1.

The following chapter will include the antibody staining process involved in confirming the presence of HS in the positive control selected for the subsequent experiments. It includes the development of the protocol including the selections for antibody dilutions. This protocol will aid future researchers with staining this cell line with these specific antibodies as it will eliminate a need to do a dilution series test, thus conserving more antibody. Chapter 4 will capture microscopy images of the development of HS within HMEC-1 over a time period. Chapter 5 then proves the presence of HS within the HMEC-1 by enzymatically degrading with heparinase.

CHAPTER 3: ENGLEBRETH-HOLM-SWARM MOUSE SARCOMA BASEMENT MEMBRANE HEPARAN SULFATE (POSITIVE CONTROL) STAINING

3.1 Abstract

This study was to confirm that the positive control, mouse sarcoma HS, did in fact react with the primary antibody selected. This would be the control for all future experiments. Three different concentrations of HS were tested as well as two concentrations of primary antibody. After staining seeded HS, it was evident as shown in the results portion of this chapter that the control did work appropriately as shown in Figures 3.2-3.5. There was no qualitatively significant difference between the

concentrations used for the HS and the primary antibody. For future experiments the more dilute primary antibody concentration was used.

3.2 Introduction

Within our blood vessels lie a thin layer of endothelial cells that serve as a barrier between blood flow and vessel wall. These cells are uniformly covered by a hydrated mesh structure known as the EGCX. The GCX is a carbohydrate rich layer that protects the cell surface from negative interactions brought upon by other immune mechanisms in response to inflammation and abnormal shear stress. These interactions can and eventually will alter the structure's ability to protect the vascular wall thus making a blood vessel more prone to disease. The GCX is formed primarily by proteoglycans and GAGs. Proteoglycans are heavily glycosylated chains consisting of GAGs. The proteoglycans work with other cell adhesion receptors and facilitate cell-cell interactions [60]. Glycosaminoglycans display many biological roles including vesicular transport, cell signaling and nitric oxide synthase [23]. The most dominant GAG on the cell surface are HS, CS, and HA. Heparan sulfate is the most abundant accounting for 50-90% of all the GAGs [7, 23, 24]. Heparan sulfate is involved in mechanisms of cell adhesion, maintaining endothelial surface layer integrity, and responding to endothelial injury [61].

The GCX can vary between a healthy and diseased state based off what physiological conditions it is currently facing [10]. During the adaptation process endothelial dysfunction ensues as a prominent feature in CVD. In CVD the GCX sheds; this in turn promotes a proinflammatory phenotype that enhances leukocyte adhesion and reduces nitric oxide production [11, 48]. This causes endothelial cells to deviate from a

state of homeostasis and become exposed to fluid shear stress. Current research investigates the protective relationship between the glycocalyx and its loss of protective properties when undergoing change in the biological environment. This change enforces the need to understand how the structure transitions from a healthy to a diseased state. Our current research aims to show how the GCX alters itself in response to mechanical stimuli which will enhance our understanding of the GCX in diseases such as CVD.

Cardiovascular disease is the main cause of mortality throughout the world at roughly 30%. The global cost put treatment and diagnoses for this disease is over 900 billion dollars [62]. Risk factors include high blood pressure, diabetes, smoking, high cholesterol as well as inheritability. Cardiovascular disease is not independently affected by genetic makeup or environmental exposure, instead it is developed consequently due to interactions between genotypes and environmental agents [63]. A precursor to most CVDs is atherosclerosis; an arterial vessel disease that occurs due to dysfunction of the endothelial cells that line the vascular wall. This disease is characterized by plaque buildups that soon progress into ruptures in the vasculature. Accumulations of plaque can initiate disruptions in blood flow inducing irregular wall shear stress and obstruction of blood flow. These issues can cause specific organs to stop functioning leading to stroke or heart attack. The GCX that protects endothelial cells serves as the first line of defense against atherosclerosis. This component is exposed to all hemodynamic forces and must mediate through the changes in the biological environment. Endothelial cells are responsible for nitric oxide production, junction interconnections and as a barrier to unwanted molecules [50]. Once the cells are dysfunctional, impairment occurs in all communication and functions. Because of these common issues, understanding the

function of endothelial cells and the GCX has been a priority in recent research to assist with treating this fatal disease.

In order to study the development of the GCX over time, it was necessary to ensure that the selected HS worked properly in conjunction with the antibodies. With this experiment being successful, this HS could be used as a positive control for future experiments to verify reliability and accuracy with the protocol. However, if unsuccessful, then more care and time would be required in select a different HS that could react with the antibodies. This preliminary test needs to be done before the GCX progression over time experimentation can take place.

For upcoming experiments to be dependable and consistent a positive control, H4777 Englebreth-Holm-Swarm mouse sarcoma basement membrane, was selected and tested. This control was sourced from Sigma Aldrich and matched with the 10E4 epitope primary antibody due to the matching species reactivity. Confirmation of reactivity with the tested HS and antibodies for future experiments is needed to verify reproducibility of protocol and upcoming test samples. Once established that the positive control can be successfully bounded to the chosen primary antibody, it can be used again throughout the course of experimentation. This experiment was a vital preliminary step before testing the HMEC-1 in which our research is focused on. Two different dilution factors were selected based off recommendations from U.S. Biological Sciences and successful testing on rat fat pad endothelial cells [54]. The concentration of the HS was also tested to determine if there was much difference in prevalence.

3.3 Materials & Methods

3.3.1 Positive Control

On the first day of the experiment fibronectin (#33016-015, ThermoFisher Scientific, Waltham, MA) was pipetted into each well of a IBIDI 24 well plate (#82406, IBIDI, Germany) at 20 ug/mL at a volume of 350 µL. This well plate was incubated in a 37° C incubator with 5% CO_2 for one hour. Once the incubation period was complete the fibronectin was removed and HS isolated from mouse sarcoma basement membrane (#H4777, Sigma Aldrich, St. Louis, MO) was added. Two concentrations were chosen to test for this experiment based off recommendations from Sigma Aldrich. The concentrations tested were 0.5 µg/mL (C_L) and 1 µ/mL (C_H).

The HS was diluted with Dulbecco's phosphate-buffered saline (DPBS) (#14190-144, Gibco, Waltham, MA) to the desired concentrations. Heparan sulfate C_L was pipetted into the wells in column 1 and C_H was pipetted into the wells in column five, column two rows three and four, column six rows three and four at 300 µL per well (see Figure 3.1 for well plate layout). The blue rows represent the negative controls and the empty rows show that nothing was added to the wells. The plate was placed in a Ziploc bag with a wet Kim wipe and then stored overnight in the fridge at 4^0 C.

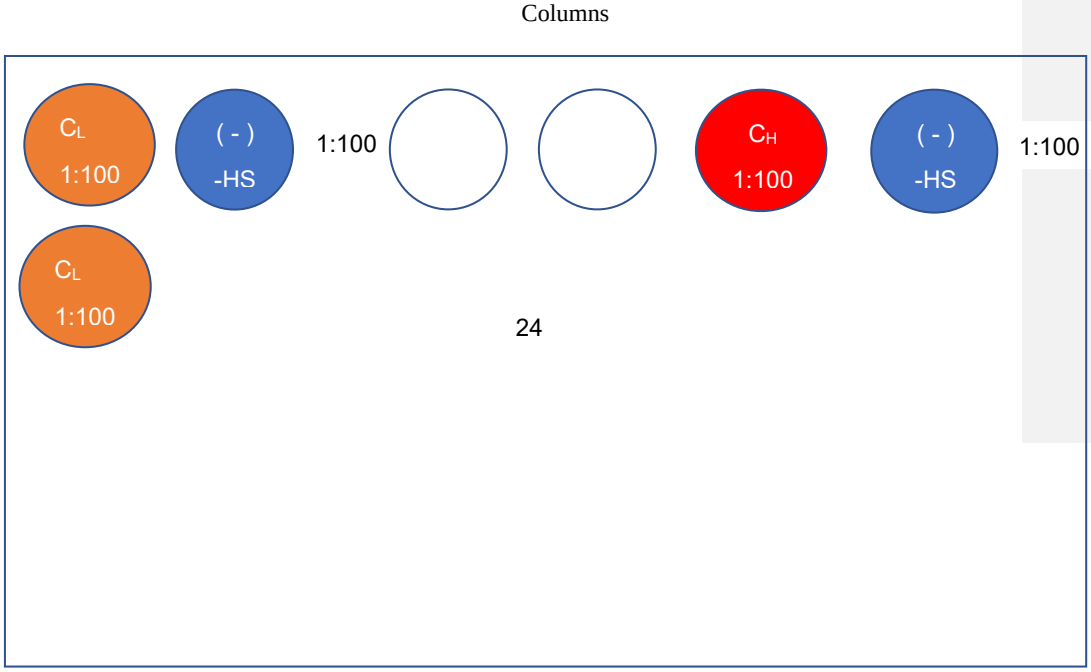

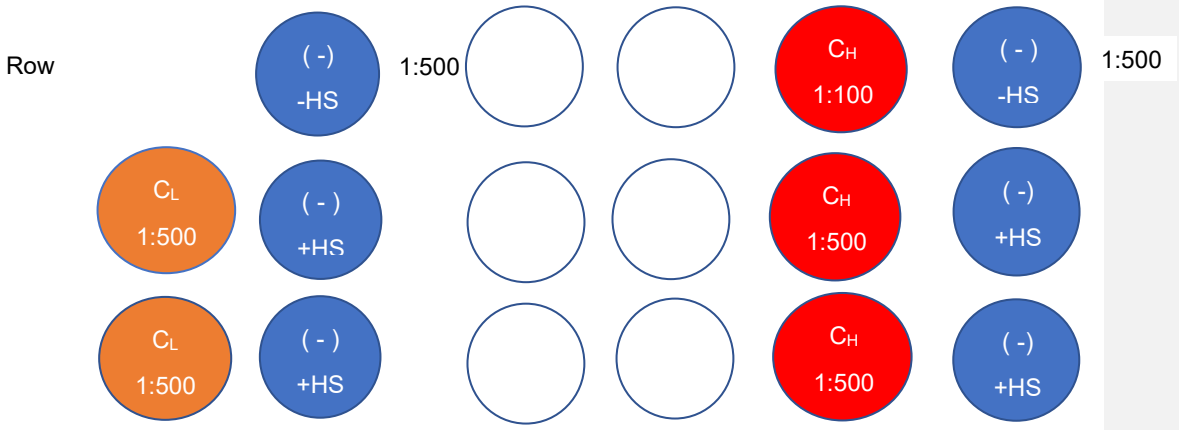

Figure 3.1: This is a schematic representation of the well plate layout. C_L signifies the lowest concentration of HS tested in this experiment. It was seeded in all wells included in column 1. C_H is the highest concentration of HS. It was put down in column 5. The 1:100 and 1:500 dilution factors correlate to the dilutions of the 10E4 primary antibody. Columns 2 and 6 were the negative controls. Those in rows 1 and 2 of columns 2 and 6 were tested to make sure that the primary antibody attached to only to HS. There wasn't any HS seeded into those wells, but they did contain the primary and secondary antibodies. Rows 3 and 4 of Columns 2 and 6 contained HS and the secondary antibody but did not include the primary antibody.

3.3.2 Immunofluorescence

The primary antibody mouse anti-heparan sulfate 10E4 epitope (#H1890, US Biological Life Sciences, Salem, MA) was diluted to a 1:100 and 1:500 ratio based off company recommendations and past research articles [54]. The antibody was diluted in solution A of 1% bovine serum albumin (BSA) (Sigma-Aldrich) in phosphate buffered saline (PBS) (#20012-043, ThermoFisher Scientific). These solutions were prepared on day two of the experimental protocol.

Once the incubation period of the HS was complete the positive control was aspirated off and 300 µL of primary antibody was added to the wells as shown in Figure 3.1. The plate was placed in the humidified chamber with a wet Kim wipe to avoid evaporation and incubated at 4° overnight. On day three of the experimental protocol the secondary antibody solution was prepared by diluting the goat anti-mouse alexa fluor 488 (ab150113, ABCAM, Cambridge, United Kingdom) with solution A in a 1:500 ratio. This solution needed to be protected from light once created. At the conclusion of the primary antibody incubation, the excess antibody was aspirated, and all the wells were washed with 350 µL of solution A three times for two minutes each. After the final wash step the wells were gently patted dry with a Kim wipe to absorb excess solution. Following these cycles, the secondary antibody was added to each of the used wells at a volume of 300 µL. The plate was placed in a Ziploc bag with a wet Kim wipe and put in an opaque box. This was stored in a dark room for two hours at room temperature. After that, the secondary antibody was aspirated from the wells and they were washed five times for two minutes each with 350 µL of solution A. After the final wash cycle the wells were gently patted dry with a dry Kim wipe. IBIDI mounting drops (#50001, Ibidi) were added to each well for immediate microscopy.

3.3.3 Microscopy

A Leica DMI 6000B inverted microscope with an HCX PL FLUOTAR 20x/0.40 Corr PH1 objective was used to acquire fluorescence images of the HS in each individual well. This setup involved a Mercury-arc lamp (#EL6000, Leica) and FITC filter cube (#11504203, Leica). Images were taken with a Leica DFC345 FX camera with a field view

of 352-μm x 264-μm. Images were acquired at 4 random positions of each well immediately following the staining process.

3.3.4 Image Analysis

The microscopy images were uploaded into Fiji (ImageJ 1.52g; Java 1.8.0_66) for image processing. First, they were converted from a 16-bit to an 8-bit with a pixel size of 352x 264 microns as advised for a more compact storage size. Not much resolution will be lost when doing this step. The brightness/contrast tool was adjusted for the images. The thresholds were maintained the same for each HS and 10E4 primary antibody concentration to keep results consistent between conditions.

Column one contained a low HS concentration (0.5μg/mL)(C_L)with a 1:100 and 1:500 ratio of the 10E4 primary antibody. Wells in column five were seeded with 1 μg/mL (C_H) HS. The images for these conditions were compared to see if there was a qualitatively substantial difference in the fluorescence signal due to the different HS concentrations and 10E4 primary antibody concentrations. The negative controls were analyzed to verify that non-specific binding between the antibodies did not take place.

3.4 Results

Select images taken from this study are shown in the figures below.

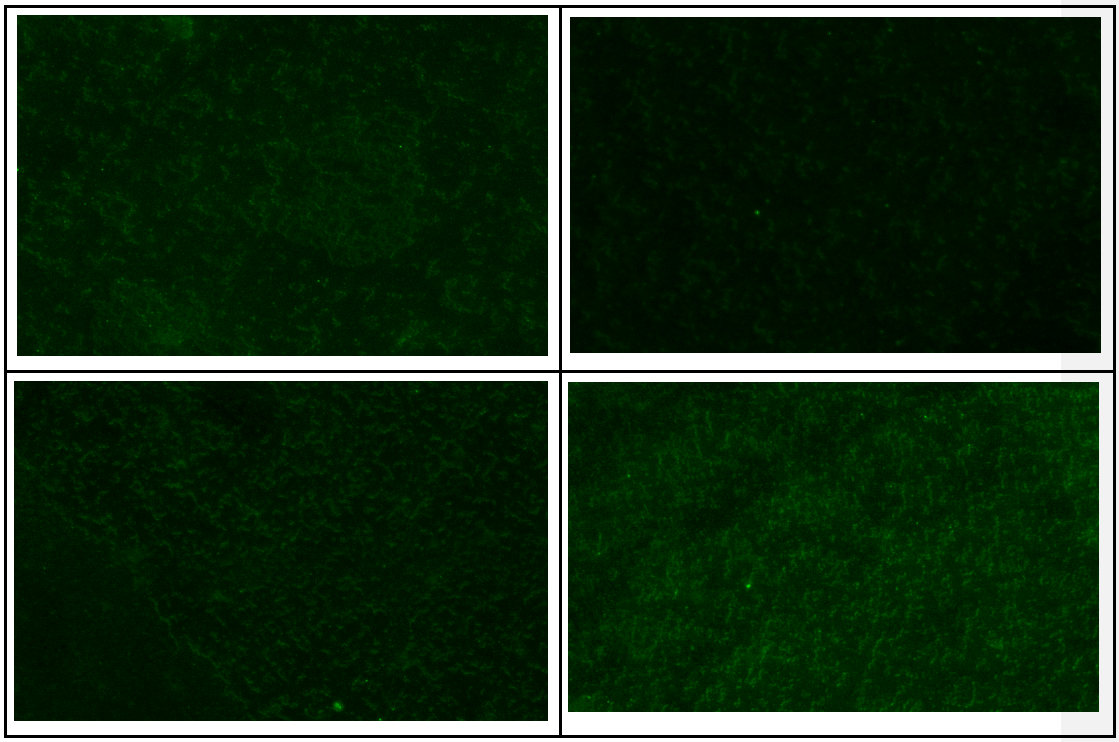

Figure 3.2**:** Fluorescence images of HS at C_L (0.5µg/mL) with a 1:100 primary antibody dilution. These images were acquired at random locations within the wells.

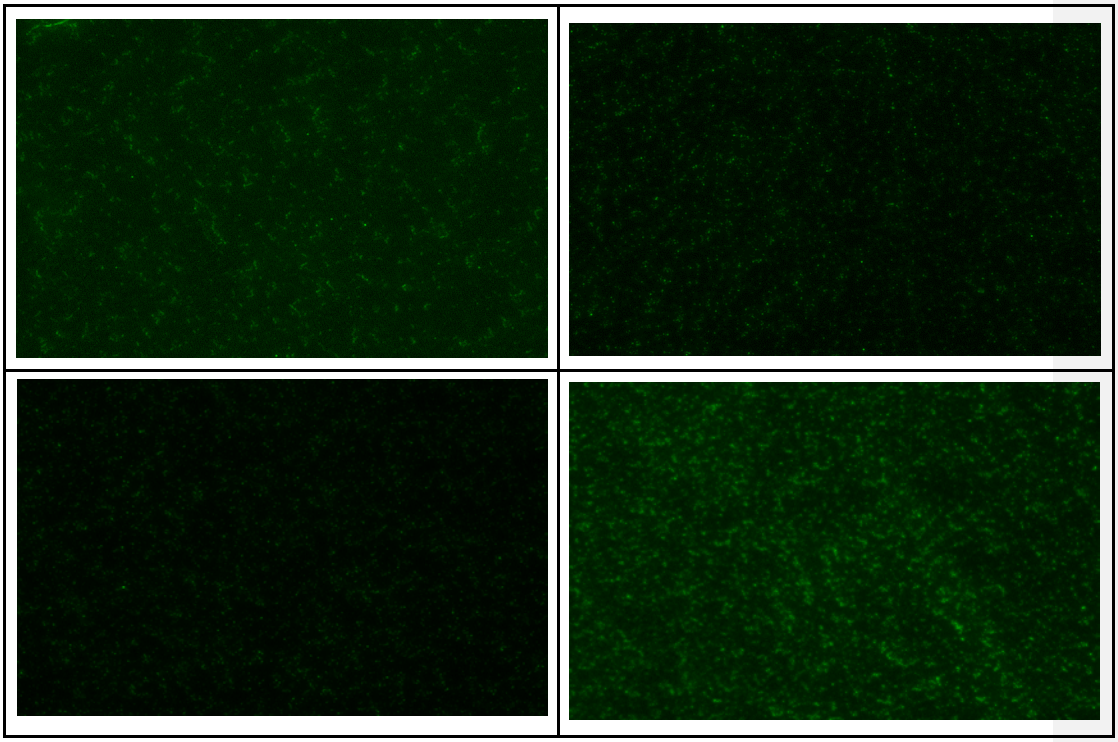

Figure 3.3: Fluorescence images of HS at C_L (0.5µg/mL) with a 1:500 primary antibody dilution. These images were acquired at random locations within the wells.

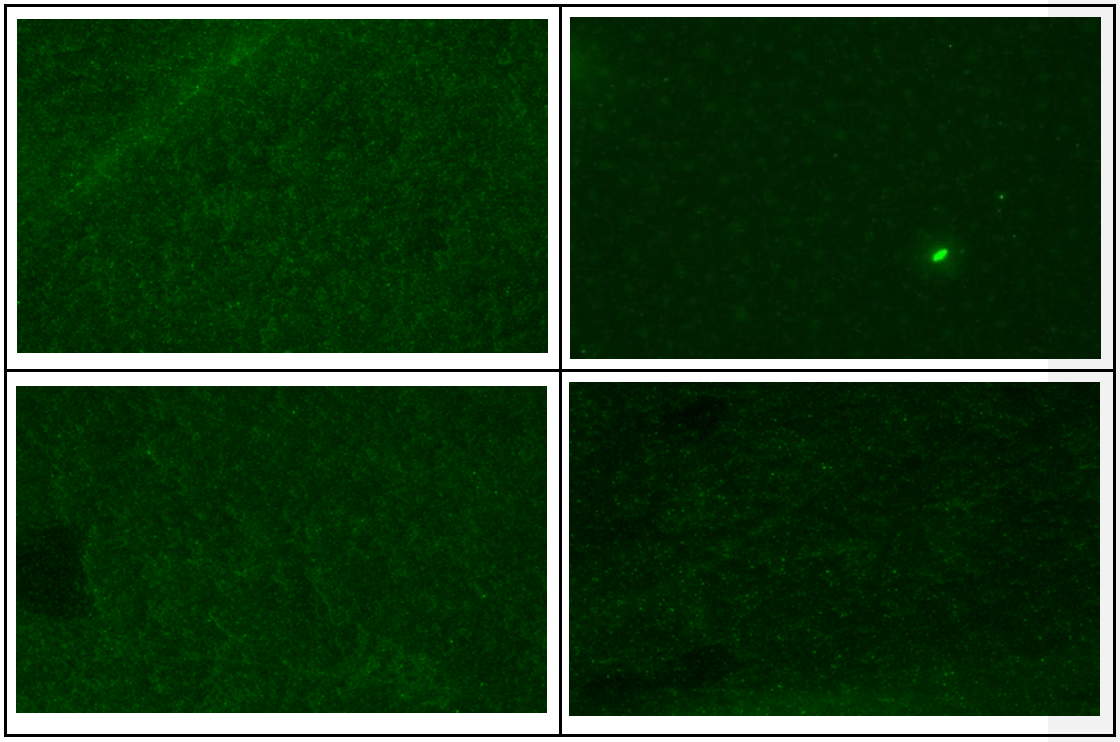

Figure 3.4: Fluorescence images of HS at C_H (1 µg/mL) with a 1:100 primary antibody dilution. These images were acquired at random locations within the wells.

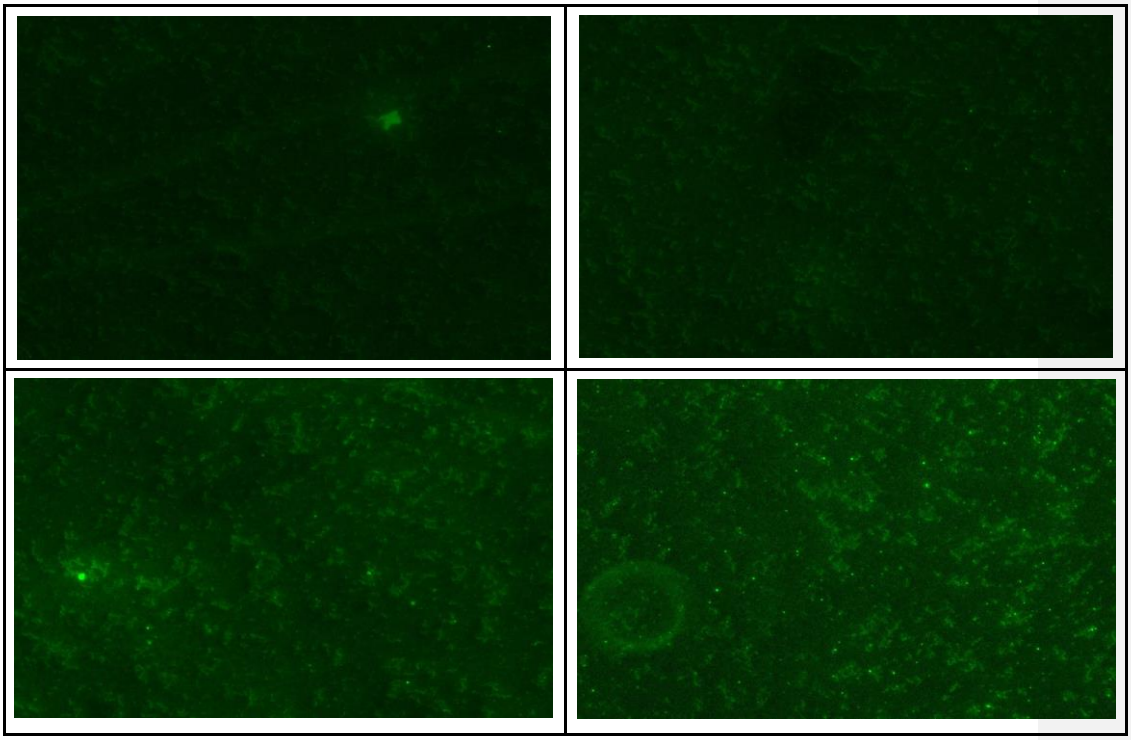

Figure 3.5: Fluorescence images of HS at C_H (1 µg/mL) with a 1:500 primary antibody dilution. These images were acquired at random locations within the wells.

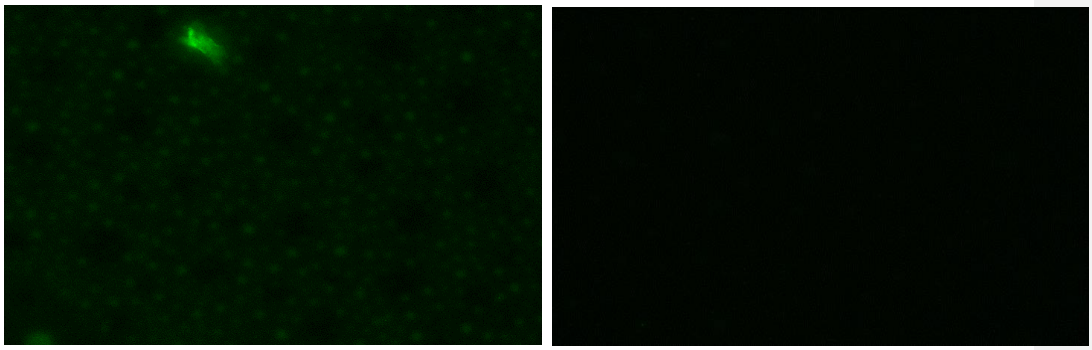

Figure 3.6: Fluorescence images of well without HS and 1:100 primary antibody dilution. These images were acquired at random locations within the well.

Figure 3.7: Fluorescence images of HS at C_L (0.5µg/mL) with no primary antibody added to the well. These images were acquired at random locations within the wells.

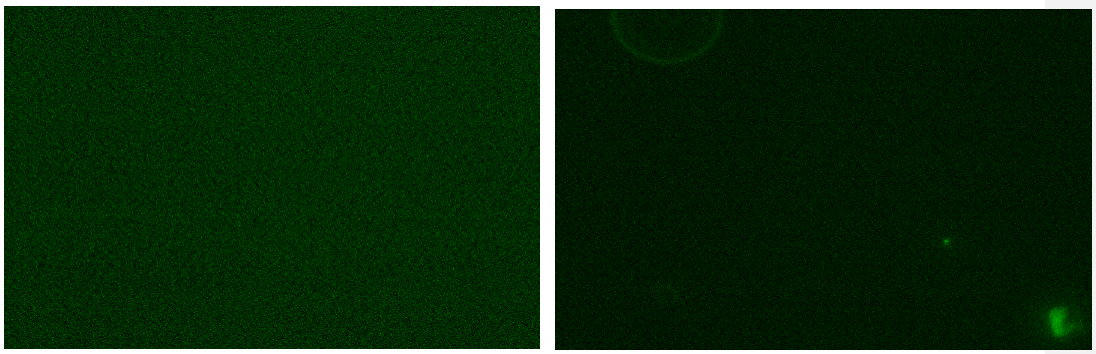

Figure 3.8: Fluorescence images of HS at C_H (1 µg/mL) with no primary antibody. These images were acquired at random locations within the wells.

3.5 Discussion

The purpose of this experiment was to verify that the HS isolated from mouse sarcoma basement membrane would indeed react with the primary antibody 10E4 epitope and be suitable to serve as a positive control. This step was crucial in that it will support future studies involving this primary antibody 10E4 epitope and HMEC-1. Based on the results from this study, the primary antibody selected did bind to the positive control mouse sarcoma basement membrane H4777.

Figures 3.2 and 3.3 represented a low concentration of the positive control mouse sarcoma basement membrane but different dilution factors for the primary antibody 10E4 epitope. As you can see from the microscopic images shown in the results section, HS was present and not visually challenging to detect. The dilution factors tested with the low concentration of positive control worked together and was evident in the images. Figures 3.4 and 3.5 shows the same dilution factors for the primary antibody 10E4 epitope but

used a higher concentration for the positive control. It appears that the HS may have a more prevalent and uniform presence than the previously tested lower concentration from Figures 3.2 and 3.3 though it was not statistically measured. Wells with no fluorescence signal were imaged and included in Figures 3.6-3.8. These negative controls were tested to show that non-specific binding occurred.

The fluorescence signal of the two different primary antibody dilutions factors tested did not visually differ. Thus, in the future we can conserve the primary antibody by using the less concentrated dilution factor or even possibly further dilute it to test whether the signal weakens.

3.6 Conclusion

The protocol established within this chapter can be utilized on HMEC-1 that are to be used in subsequent experiments. The HS chosen was successfully marked with primary and secondary antibody showing a positive reaction between the antibodies and the target. With the dilutions of primary antibody tested we can preserve primary antibody in the future by testing with the more diluted concentration.

Chapter 4: TIME SERIES EXPERIMENT STUDYING THE EVOLUTION OF HEPARAN SULFATE ON HMEC-1

4.1 Abstract

The GCX has been shown in other cell lines to develop over a course of time. The GCX begins development around the outside of the cell in the earlier days of culture. Over time, the spatial GCX distribution on the apical area of the cell changes. It is predicted that as it develops, it begins to fulfill its role in function within the body. Though this has been studied in other cell lines, HUVEC and rat fat pad endothliela cells, there has been no documentation of the spatial and temporal distribution on the HMEC-1 cell line. These experiments were designed to show how the GCX develops around the cell over a course of time. Images and z-stacks were acquired and processed in Image-J software. Early in the culture (by 3 days post-seeding), the GCX is more concentrated near the periphery of cells. However, the longer the cells are in culture the GCX spatial distribution begins to cover the entire cell. This research agrees with past research done on other cell lines [53]. For future studies, development of the GCX can be tested by use of Youngs modulus to see if it fluctuates in response to growth patterns.

4.2 Introduction

The GCX has been proven to shed and regenerate while undergoing biological processes and dysfunction. Unfortunately, in CVD this self-regulation becomes compromised and the GCX cannot regenerate at the same rate as to which it is degrading causing endothelial cell health to decline. Without the GCX, the cell could lose

functionality and become dysfunctional. Inflammation can occur and cause leukocytes to adhere to the cells [11, 53]. Reverse research was explored in this experiment and involved studying the development of the major component within the GCX. This can lead to information regarding the regeneration of shedding components within the GCX to better understand the rate and process of GCX abnormality [3]. With this knowledge it may be possible to discover ways in order to improve the regeneration rate, how to protect the GCX from regressing further, and encourage treatment. The first step is determining how long it takes the GCX to develop after initial culturing in the well plates. Similar research was done previously by Henderson-Toth, Bai and Tarbell with different cell culture and animal models at different measurements of time [53, 54, 64]. For example, Henderson-Toth imaged quail embryos at different phases of life while Bai studied HUVECs using days post seeding [53].

With this current project, it will be determined how long it will take for the most abundant constituent, HS, to develop in the GCX. Heparan sulfate lies on the surface of endothelial cells comprising of over 50% of the GAGs [12, 54]. Though it is not encompassing of the GCX in its entirety, this is still important as it can give a good inclination as to the rate and pattern at which the GCX will develop after shedding when undergoing biological stresses. Selecting time frames that are too soon before complete spatial distribution could involve a GCX that is unable to complete its role in regulating endothelial cell functions [11, 53]. The first time point for the current experiment was selected based off results from the previous work mentioned [12, 53, 64]. The following time points (4.5, 6, 7.5 days post seeding) were dictated by the resulting images from the first time point (3 days post seeding).

4.3 Materials & Methods

4.3.1 *Preparing Complete Growth Media*

Fibroblast growth factor L-glutamine and penicillin/streptomycin were added together and gently mixed in a sterile conical tube. The final concentration of the growth media was 10% fetal bovine serum, 2mM of L-glutamine, and 100U/mL /100µg/ml of penicillin/streptomycin. More details are in the protocol found in the Appendix section on page 77.

4.3.2 Handling Procedure for frozen Cells

Refer to “Handling Procedure for Frozen Cells” protocol page 80 in the Appendix for a more detailed outline of steps. A vial of frozen cells was removed from the cell chamber and thawed in a water bath. Once the vial thawed the cells were removed and media was added in aseptic conditions, it was then prepared for centrifuging. Centrifugation allowed the cells to form a pellet at the bottom of the conical tube. The excess media was removed from the top and discarded.

Cells were to be seeded in the wells at 10,000 cells/cm^2. The calculated volume of complete medium of 6.5 mL was added and mixed with the cell pellet to get approximately 56 cells/µL. Finally, 180 µL of cell medium solution was added to each well. These well plates were placed in the incubator for the predetermined number of days before removing for fixation and staining (3, 4.5, 6, 7.5 days post seeding). Cells received fresh growth media and the confluence was evaluated every day.

4.3.3 Positive and Negative Controls

As described in our previous experiment, two concentrations (0.5 and 1 µg/mL) of pure HS (H4777, Sigma Aldrich) were tested to determine what concentration gave a strong signal while also conserving reagents. When referring to our results we determined that for future experiments we would dilute HS at 0.5 µg/mL. This lower concentration appeared to not a qualitative difference signal based off the images taken of the different concentrations. For the current experiment three positive and negative control µ-slides were designed to have wells with HS and wells without. The wells intended to include HS were seeded at 0.5 µg/mL. Wells in columns one and two shown in Figure 4.1 served as positive controls to test that the primary antibody does indeed attach to the target (HS) and non-specific binding doesn't take place. Select wells as shown below in Figure 4.1 in column four did not include HS but did include both primary and secondary antibodies. This type of negative control was designed to test the antibodies reactivity to each other as well as to the absence of the HS. It needs to be confirmed that the primary antibody does not attach to anything else but the pure HS; therefore, there should not be a signal. Column three served as another form of negative control but verified that the secondary antibody only attaches to the primary antibody. With no primary antibody present in these wells there should not be a signal detected. These µ-plates were all prepared one day before each time point plate was fixed and stained. The working volume for the solutions and antibodies were 150 µL.

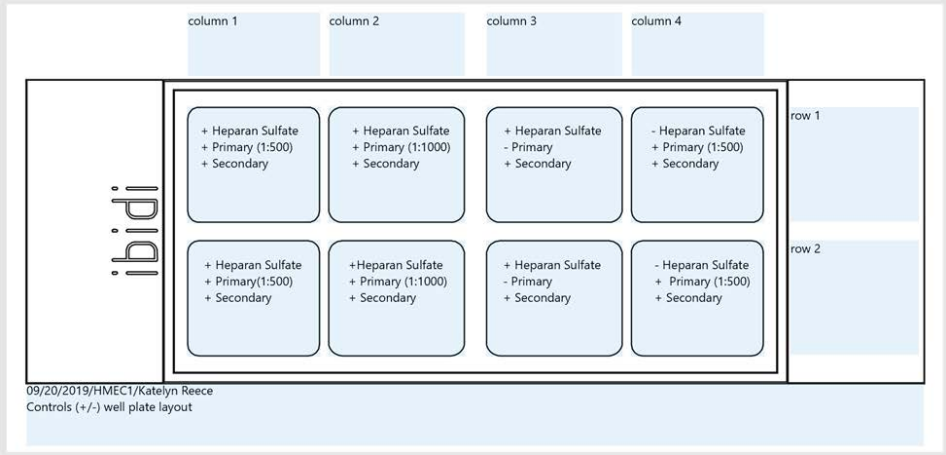

Figure 4.1: This is a schematic representation of the µ-plates layout for the HS positive and negative controls.

4.3.4 Preparation of 4% PFA

Refer to “Preparation of 4% (w/v) Paraformaldehyde in PBS” protocol in the Appendix section for full list of materials and methods. Approximately 2 ml of paraformaldehyde solution was prepared two days post 100% confluence for this experiment. Paraformaldehyde was weighed out at 0.08 grams and added to 2 mL of heated PBS to reach 4%. Once the solution cooled, it was filtered, and the desired pH was reached using hydrochloric acid and sodium hydroxide.

4.3.5 Time Points

Once 100% confluence was reached, three days' time was waited before removing from the incubator one well plate containing HMEC-1. The day prior to HMEC-1 well plate removal, the positive/negative control plate was prepared as described previously in the positive and negative controls section of the methods. The HMEC-1 plate and corresponding control plates were then prepared for fixation and staining. Additional other prepared HMEC-1 well plates were removed from the incubator and fixed at time points 4.5, 6, 7.5 days post seeding the cells into the wells. Figure 4.2 features a schematic representation the well plate layout for the HMEC-1 plates. One day prior to each HMEC-1 plate removal, the control plates as shown in Figure 4.1 were prepared. These time points (3, 4.5, 6, 7.5 days), were determined based off images obtained from the μ-well plate at time point 1 (3 days post 100% seeding) and past research [53].

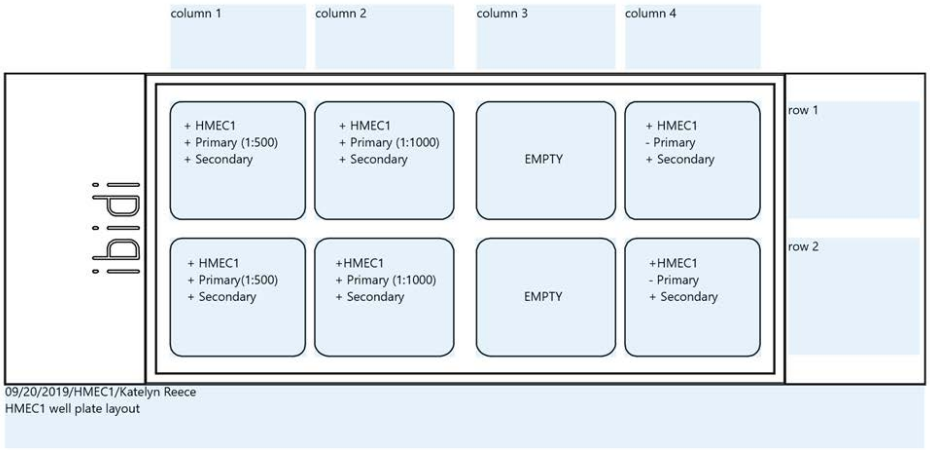

Figure 4.2: This is a schematic representation of the µ-plates layout for the HMEC-1. This layout was mimicked for all four µ-plates that contain HMEC-1. The entire first column was used to test the more concentrated dilution of primary antibody (1:500) on the cells. Column 2 tested the primary dilution factor (1:1000). Column 3 was purposely left empty without cells nor antibodies. Column 4 served as a negative control with HMEC1 and secondary antibody but no primary antibody.

4.3.6 Staining protocol for HMEC1 in u-slide 8 wells

Once HMEC-1 well plates were removed from the incubator, cells were washed with pre-warmed PBS and fixed with previously prepared 4% PFA for approximately 10 minutes. Primary and secondary antibodies were added post fixation at 150 µL per well. Cells were then washed with PBS again and mounted in IBIDI mounting drops.

Refer to “Staining of HMEC-1 in µ-slide 8 Wells” protocol on page 85 in the Appendix section for further in-depth details.

4.3.7 Microscopy Imaging

A Zeiss Primovert inverted light microscope with a 10x/PH1 and 20x/PH1 objective was used to monitor the confluency of HMEC-1 well plates. Confluency was tracked predominantly in the center of the wells as most cells tend to congregate in the middle of the well vs the outer edges.

A Leica DMI 6000B inverted microscope with a HCX PL FLUOTAR 20x/0.70 Corr PH1 objective was used to acquire fluorescence images of the HS that lies within the HMEC-1 and also of the HS controls. This setup involved a Mercury-arc lamp (#EL6000, Leica) as well as a DAPI and FITC ET filter cube (#11504203, Leica). Images were taken with a Leica DFC345 FX camera with a field view of 352-μm x 264-μm. Images were acquired at three randomly selected positions of the selected wells based off a random number generator formula (=RANDBETWEEN(1,9) created in Excel. The wells were divided into nine different regions and three locations were selected from those regions.

A confocal microscope(A Zeiss Primovert inverted light microscope) was utilized for acquiring z-stacks at three random locations based off the random number generator created in Excel. For acquiring z-stacks the Δz was set to 0.5 μm. This was selected based off past research documenting the assumed thickness of the GCX in a range of several hundred nanemeters to a few micrometers [16, 53]. The beginning and end positions varied with each random position selected within the well and was not consistent between the locations. The number of slices captured also varied depending on the distance selected between the two points. The format for the setting was 1600 x 1600.

The scan speed was set to 400 Hz. The pixel size 85.45 nm x 85.45 nm. The pinhole was set to 95.63 µm AIRY units. The line average was 6 for HS and 2 for the nucleus.

4.3.8 Image analysis

The microscopy images were uploaded into Fiji (ImageJ 1.52g; Java 1.8.0_66) for image processing. First, they were converted from a 16-bit to an 8-bit with a pixel size of 352x 264 microns. The brightness/contrast tool was adjusted for the images. For the "controls" µ-well plates, the thresholds were maintained the same for each separate section containing HS (H477, Sigma Aldrich). For those that served as the negative controls in the "controls" µ-well plates, each concentration of primary antibody (1:500 and 1:1000) had its own consistent threshold. For the well plates analyzed at the time points, thresholds were kept consistent for each separate concentration of primary antibody (1:500 and 1:1000). This method was used to keep results and image quality consistent.

The widefield z-stack images were also uploaded into Fiji but no image processing or adjustments were done with the brightness/contrast tool. The slices were projected down into three different selected projections with a pixel size of 1600 x 1200 microns. The selected z projections were maximum intensity, average intensity and sum of the slices.

4.4 Results

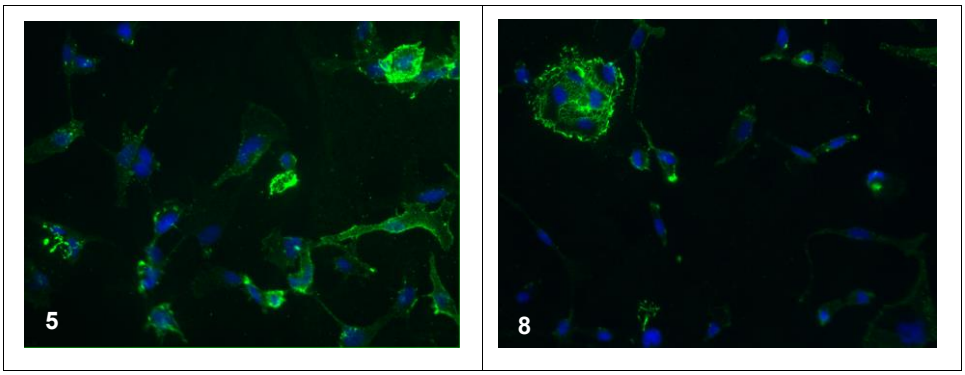

Figure 4.3: Widefield images of well in column 1 row 1 of layout depicted in Figure 4.2. The cells were fixed and stained 3 days post seeding. The generated locations are location 5 (middle of well) and 8 (lower middle of well).

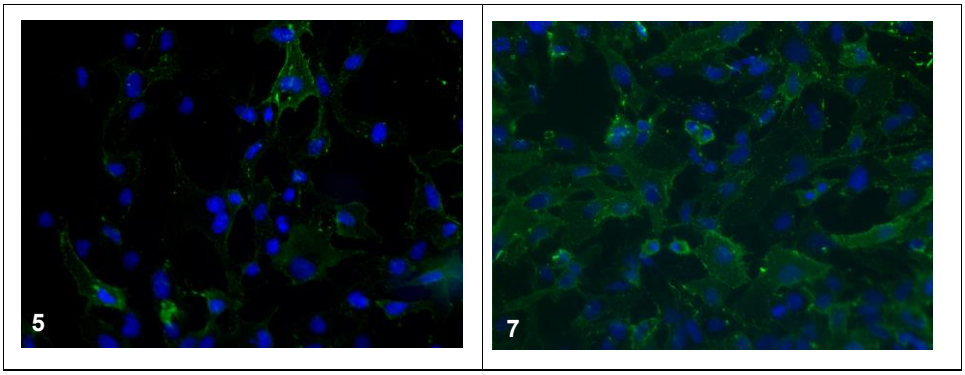

Figure 4.4: Widefield images of well in column 1 row 1 of layout shown in Figure 4.2. These cells were fixed and stained 4.5 days post seeding. The presented locations are 5 (center of well) and 7(lower left corner of well).

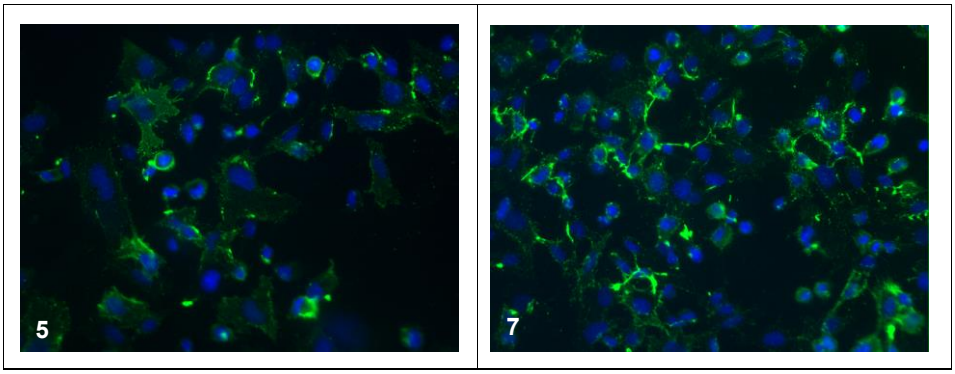

Figure 4.5: Widefield images of well in column 1 row 1 of layout shown in Figure 4.2. The cells were fixed and stained 6 days post seeding. The images shown were taken from locations 5 (middle section of well) and 7 (lower left corner of well).

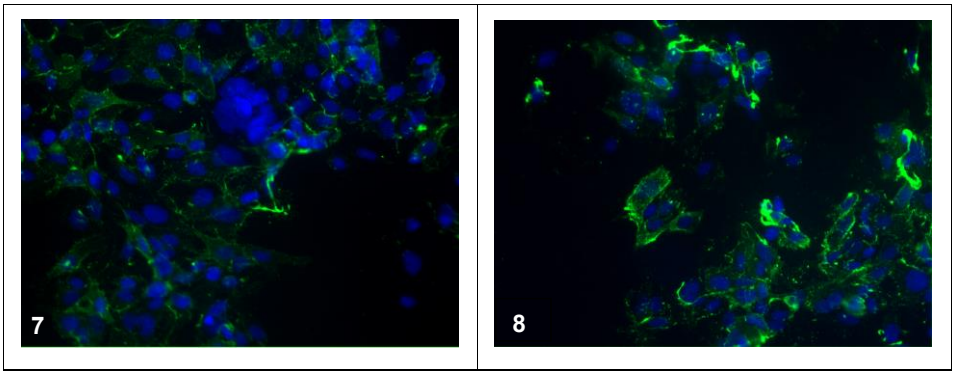

Figure 4.6: Widefield images of well in column 1 row 1 of layout depicted in Figure 4.2. These cells were fixed and stained 7.5 days post seeding. The locations generated for this plate were 7 (lower left corner) and 8 (lower middle section).

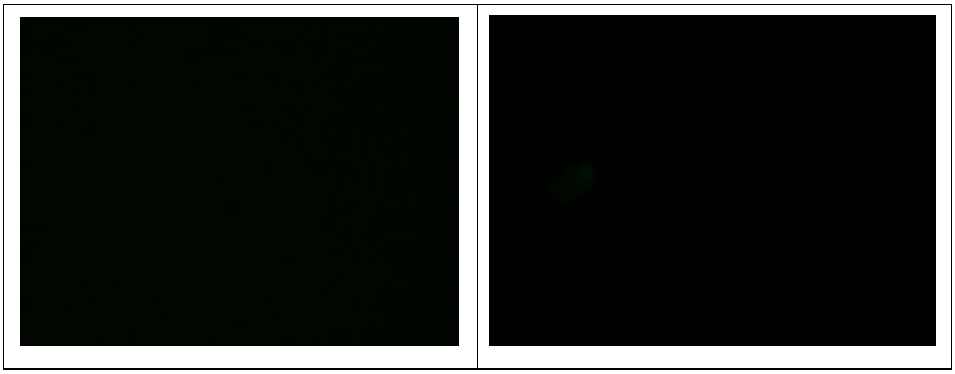

Figure 4.7: Widefield images of negative controls in which no primary antibody was used therefore no reaction was to take place.

Maximum	Sum	Average
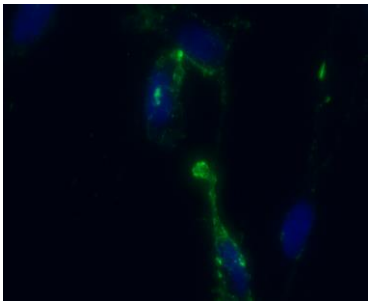	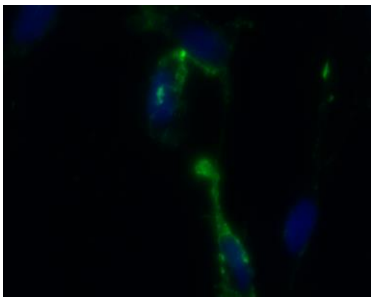	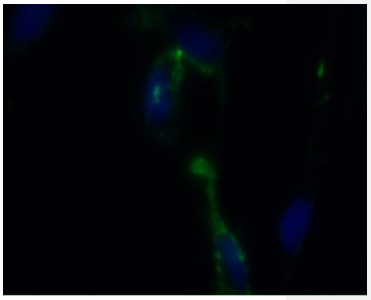

Figure 4.8: Widefield Z-stacks of location 5 in well in column 1 row 1 of Figure 4.2 three days post seeding. Shown are Z projections maximum intensity, sum, and average intensity.

Maximum	Sum	Average
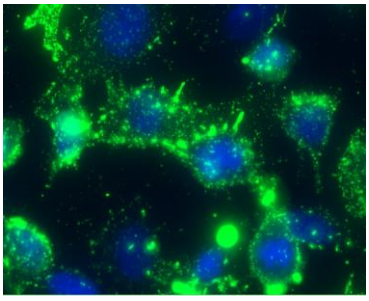	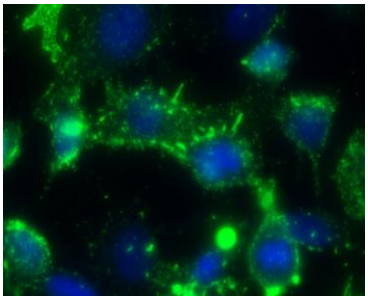	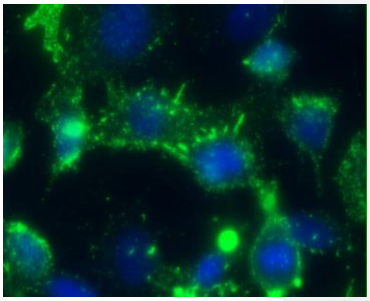

Figure 4.9: Widefield Z-stacks of location 5 in well located at position column 1 row 1 represented in Figure 4.2 six days post seeding. Selected Z projections are shown.

4.5 Discussion

Based off the images displayed in Figures 4.3-4.6 it is assumed that more HS developed over the course of time. The widefield microscopy images displayed in Figure 4.6 showed the greater abundance of heparan sulfate in comparison to the images shown in Figure 4.3. However, there was no measuring instrument used for this other than the visual tool, the microscope. It was kept in mind that not only did the rate of heparan sulfate develop but also the number of cells multiplied as well. When visually evaluating the results after image processing, an area of approximately ten nuclei was selected and observed in order to determine whether HS development did in fact transform around the cells over time. The sample size of 10 was selected due to many regions of the well having cells clumped together. A better representation of this can be seen in Figures 4.8 and 4.9. The Z-stacks shown in Figure 4.8 represent how the HS developed 3 days post

seeding. It is apparent that not every cell had HS around it at this time. Also, it appears that the HS that was present, did not fully encompass around the cells. In Figure 4.9 it is shown that HS is surrounded by numerous if not all the cells imaged. The HS distributed completely around the cell and not just near the outer endothelium but also towards the apical area.

These results do agree with research completed on HUVECs involving the development of HS and HA. Similar distribution patterns were shown with the GAGs developing along the outer edges in days 3 and 5 post culture. By day 7.5 the HS appeared to have traveled over the entire membrane [53].

4.6 Conclusion

Results from this experiment show that the HS developed across the HMEC-1 did follow a similar pattern to that of HUVECs by first appearing around outer edges of the cell near the cell borders before traveling towards the nucleus and over the entire epithelium [3, 53]. Understanding why the distribution occurs on the outside of the endothelium followed by near the cortex will need further investigation. As HS develops across the cells and along the borders between cells, the greater the intercellular communication [3]. It might be beneficial to also measure the thickness of the GCX using atomic force microscopy to see how it varies over the course of selected days. The thickness of the GCX, as well as other additional factors, can give insight as to how permeable the GCX is. Research increasing time intervals might give a more accurate

representation of how HS progresses. Despite this, the current study provides an optimistic representation for HS development in HMEC-1.

Chapter 5: ENZYME DEGRADATION OF HEPARAN SULFATE ON HMEC-1

5.1 Abstract

HMEC-1 were cultured for 6 days post seeding and then enzymatically degraded with heparinase III. Once enzymatic treatment was complete, cells were then fixed and stained for HS and the nucleus. After imaging, it was shown that HS degraded away sequentially in response to the increasing enzyme concentration. The results show that HS does lie within the GCX encompassing the HMEC-1. If this experiment was replicated in the future, a greater concentration of enzyme would be used.

5.2 Introduction

Lifestyle choices made by the world's inhabitants have unfortunately led to many being in a diseased state. This diseased state can be the outcome of poor nutrition and lack of exercise ultimately leading to CVD [62]. Cardiovascular disease can fatally harm the heart and blood vessels. Our blood vessels are lined with endothelial cells which form an interface between the lumen and the vessel wall. Due to their location, endothelial cells are exposed to hemodynamic forces that induce alterations. When healthy, endothelial cells contain a complete mesh-like structure referred to as the GCX. This network is made up of glycoproteins and proteoglycans and is responsible in vascular physiology for maintaining homeostasis, cell-to-cell interactions, and permeability. Over time, the GCX sheds and is a dynamic structure that can transition to a diseased state [7, 63].

The most prominent component within the GCX is the GAG HS. Heparan sulfate has been found to be correlated to nitric oxide production and signal transduction [23].

Heparan sulfate is the focus of this study as the goal is to prove that what we are claiming to be present on HMEC-1 is indeed HS. This GAG has been confirmed on other cell lines such as rat fat-pad endothelial cells, bovine aortic endothelial cells, HUVECs, human coronary artery endothelial cells, by enzymatic degradation or shear applications [2, 13, 53, 65]. Past research was developed not only to show that HS was present, but also to measure its role within the GCX after removal. Ebong et al. studied how after being exposed to fluid shear stress, HS tended to form “clusters” in a nonuniform pattern. It Is hypothesized that this clustering behavior can recruit signaling molecules that can impair vasodilation within the vascular wall leading endothelial cells to conform to a diseased state [66].

With this current study, the goal is to prove through enzymatic degradation that HS lies within HMEC-1. This has not been proven on this cell line before and can give insight as to what other proteoglycans or GAGs constitute the GCX in this cell line. With success in this research future works can include measuring nitric oxide production or the GCX’s role in mechano-transduction after HS elimination. This experiment will include testing different enzyme concentrations, heparinase III, to determine if there is a qualitative difference. The concentrations selected are based off what has been found to be successful in previous research [11, 53, 64, 65, 67, 68].

5.3 Materials & Methods

5.3.1 Preparing Complete Growth Media

The protocol in the Appendix section was utilized in making 10% FBS, 2mM L-Glut, Pen/Strep growth media. Fibroblast growth factor, L-glutamine and penicillin/streptomycin were added together to reach the final needed volume of approximately 7 mL. This growth media was used to provide nutrients to the cells over the course of time. Old media was exchanged with new media every 24 hours after confluency was estimated. Full list of methods and materials are in Appendix section.

5.3.2 Handling Procedure for frozen Cells

Refer to “Handling Procedure for Frozen Cells” protocol page 80 of Appendix for full outline of steps. Values decided on specifically to this experiment are mentioned as followed. Cells needed to be seeded at 10,000 cells/cm^2. The frozen vial of cells was removed from the cell chamber and thawed in a water bath at 37^o C. The calculated volume of complete medium was added to the cell pellet to get approximately 56 cells/µL. Finally, 180 µL of cell medium solution was added to each well. These well plates were placed in the incubator for 6 days (2 days post 100% confluence). Cells received fresh media and the confluency was evaluated every day.

5.3.3 *Positive and Negative Control*

Refer to “Positive Control Heparan Sulfate Staining” protocol on page 81 of Appendix for a more detailed list of materials and methods. As described in chapter 3, two concentrations (0.5, 1 µg/mL) of pure HS H4777 were tested. It was determined that for future experiments we would conserve the HS by using the 0.5 µg/mL concentration. For the current experiment only one positive and negative control µ-slides was needed. The wells intended to include HS were seeded at 0.5 µg/mL. Wells in columns one shown in Figure 5.3 served as positive controls to test that the primary antibody attaches to the target (HS) and non-specific binding doesn’t occur. Select wells as shown in Figure 5.3, column four did not include HS but did include primary and secondary antibodies. This negative control was planned to confirm the antibodies’ reactivity to each other as well as to the absence of the HS. Column three served as alternative form of negative control but tested that the secondary antibody only attaches to the primary antibody. These µ-plates were all prepared one day prior to the fixation of the HMEC-1 plates. The working volume for the solutions and antibodies were 150 µL per well.

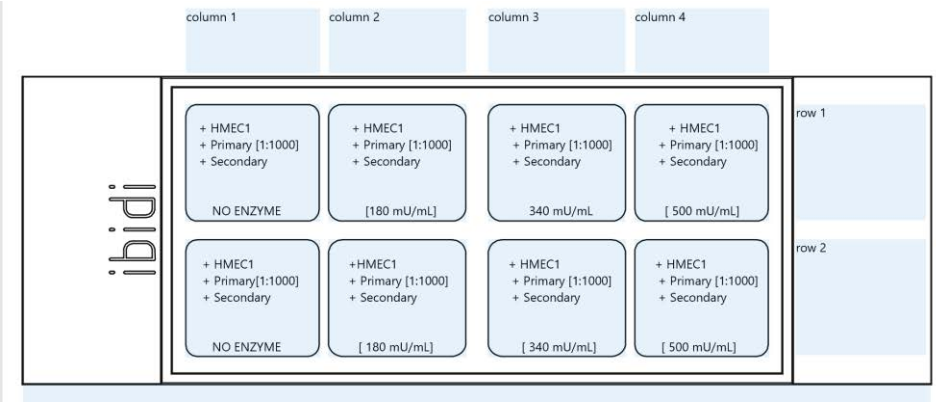

Figure 5.1 schematic representation of well plate layout for HMEC-1 enzymatic degradation. The primary antibody concentration was kept constant at 1:100 dilution. The first column did not contain any enzyme. The second column was tested with 180 mU/mL, the third column with 300 mU/mL and the final column with 500mU/mL.

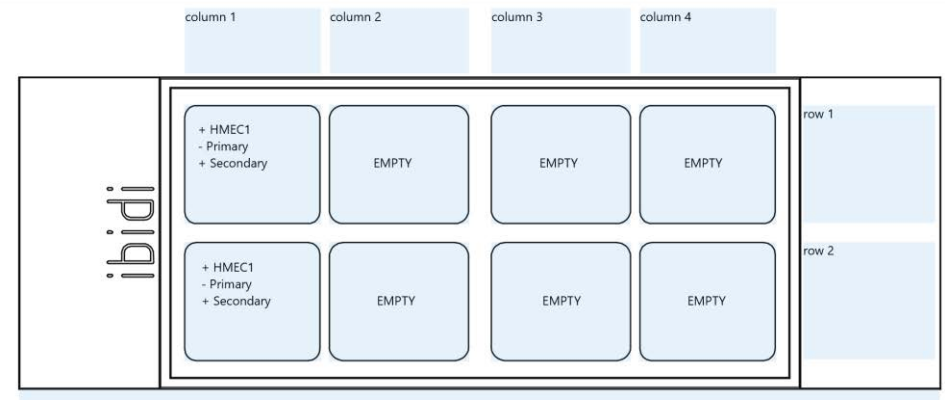

Figure 5.2: Well plate layout for HMEC-1 negative controls. Column 1 contained no primary antibody, so no reactivity was to take place.

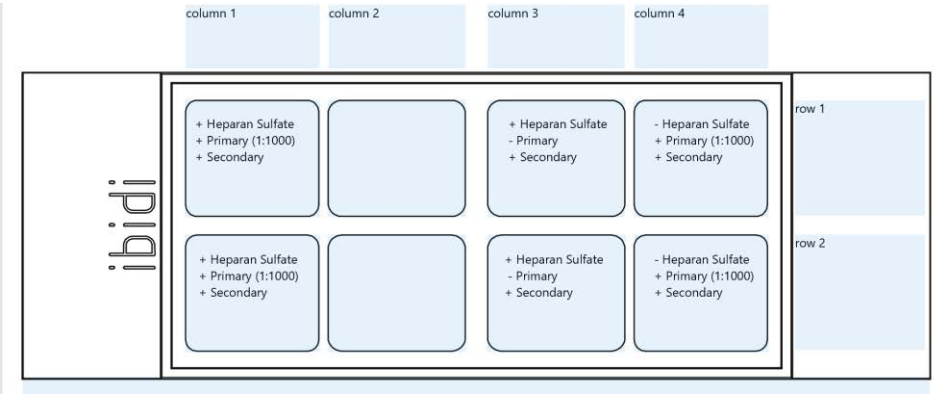

Figure 5.3: Well plate layout for +/- controls. Column one served as the positive control with the same primary antibody concentration as in the HMEC-1 plate. Column two was left intentionally empty. Column three and four served as negative controls.

5.3.4 Preparation of 4% PFA

"Refer to preparation of 4% (w/v) Paraformaldehyde in PBS" protocol of Appendix on page 83 for complete list of materials and methods used. Paraformaldehyde powder (0.08g) was added to 2 mL of PBS on a heating/stirring plate. The final pH was adjusted by use of HCl and NaOH. Paraformaldehyde solution was prepared 3 days post seeding for this experiment.

5.3.5 Enzymatic Degradation

Heparinase III aliquots (0.5mL) were previously diluted into serum free media to reach the concentration (500mU/mL) for storage in the freezer. When ready for use the aliquots were removed from the freezer and again diluted with serum free media to reach

the three different desired concentrations of 180, 340, and 500 mU/mL. The prepared heparinase III was added to each intended well at 150 µL. The HMEC-1 cells were then incubated for two hours. Once the time point was reached, the cells were then washed with PBS three times for five minutes each. Once enzymatic degradation was complete the cells were then fixed with 4% PFA for ten minutes at room temperature.

Refer to “Enzymatic Degradation of HMEC1” protocol in the Appendix for further details. The enzyme concentration increased sequentially throughout the columns in the well plate shown in figure 5.3.

5.3.6 Staining protocol for HMEC1 in u-slide 8 wells

After fixation, the cells were washed with a washing buffer of 0.1% BSA in PBS. A blocking buffer was created including 132 µL of goat serum and 0.3 grams of glycine to reach the needed volume of approximately 1.5 mL. A primary antibody was made by adding 1.815 µL of the stock to 1.81 mL of the washing buffer. The blocking solution was then added to the cells for 30 minutes at room temperature. The blocking buffer was aspirated from the wells and a primary antibody was added to each well at 150 µL. The well plates were stored in an opaque box and put in the fridge overnight at 4^0C. Once incubation period was reached, the well plates were removed from the fridge and the cells were washed with the washing buffer. The secondary antibody was added to each intended well of cells at 150mL and stored in a dark space for two hours. During the incubation period a Hoechst stain was made by mixing 1.65 µL from the stock with 1.6 mL of the washing buffer. Once two hours was reached, the secondary antibody was removed, and the Hoechst dye for the nuclei was added for five minutes at room

temperature. Cells were washed and finally a mounting drop was added to each well before imaging could occur.

Refer to “Staining of HMEC1 in µ-slide 8 Wells” protocol on page 85 of the Appendix section for further details.

5.3.7 Microscopy Imaging

A Zeiss Primovert inverted light microscope with a 10x/PH1 and 20x/PH1 objective was used to monitor the confluency rate of the HMEC-1 well plates shown in figures 5.1 and 5.2. Confluency progress was tracked predominantly in the center of the wells.

A Leica DMI 6000B inverted microscope with a HCX PL FLUOTAR 20x/0.70 Corr PH1 objective was used to acquire fluorescence images of the HS and nuclei that lie within the HMEC-1 cells. Images were also acquired of the positive and negative controls. This setup involved a Mercury-arc lamp (#EL6000, Leica) , DAPI and FITC ET filter cube (#11504203, Leica). Images were taken with a Leica DFC345 FX camera with a field view of 352-µm x 264-µm. The images were captured at random locations within wells of row 1 columns 1-4 that were chosen by a random number generator formula written in Excel.

Commented [RK1]: Will need to change when experiment completed if it changes

Commented [RK2]: Would like this rewritten

5.3.8 Image analysis

The flat plane widefield microscopy images were uploaded into Fiji (ImageJ 1.52g; Java 1.8.0_66) for image processing. First, they were converted from a 16-bit to an 8-bit with a pixel size of 352 x 264 microns. The brightness/contrast tool was adjusted for the images. For the “controls” µ-well plates, the thresholds were maintained the same for

each separate section containing HS (H477, Sigma Aldrich) as well as for those that did not. For the HMEC-1 well plates, thresholds were kept consistent for each separate concentration of enzyme. This method was used to keep results and image quality consistent.

The widefield z-stack images were uploaded into Fiji but no image processing or adjustments were done with the brightness/contrast tool. The slices were projected down into three different selected projections with a pixel size of 1600 x 1200 microns. The selected z projections were maximum intensity, average intensity and sum of the slices. The three z projections were chosen based off the need to give the most precise and encompassing image quality with no outlier fluorescents obscuring the results.

5.4 Results

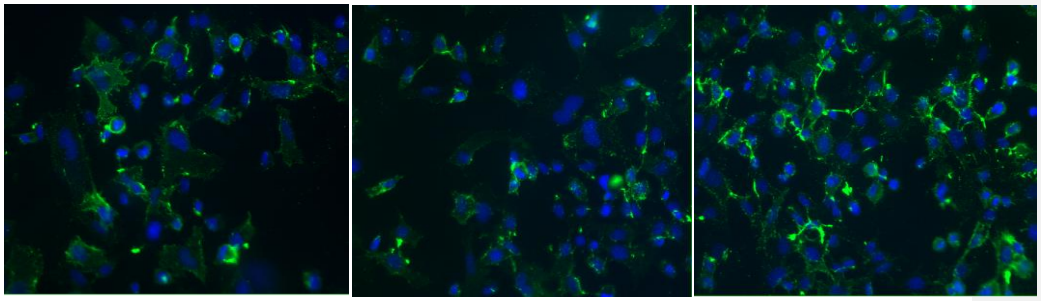

Figure 5.4: Widefield images of cells in well located at column 1 row 1 of Figure 5.1. This well does not contain an enzyme and displayed are locations 5, 6, 7.

Average	Maximum	Sum
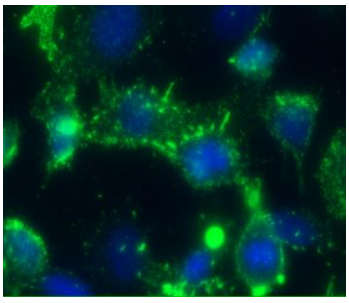	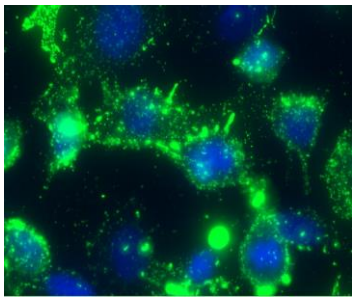	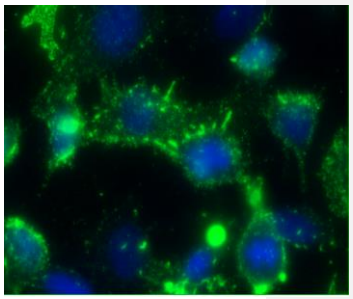

Figure 5.5: Widefield Z-stacks of location 5 of cells in column 1 row 1 of Figure 5.1. This well does not contain an enzyme. No degradation took place.

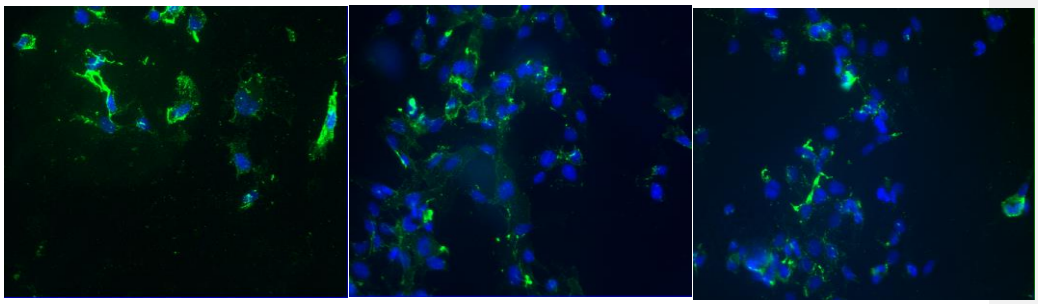

Figure 5.6: Widefield images of cells in well located in column 2 row 1 in figure 5.1. This well was treated with 180mU/mL of the enzyme heparinase III. Degradation did take place. Figure includes locations 5-7.

Average	Maximum	Sum
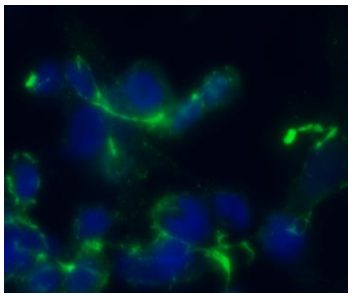	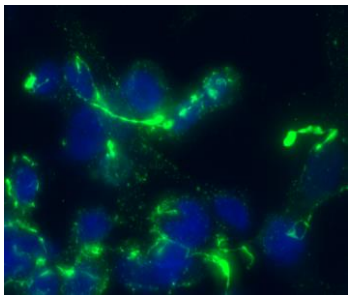	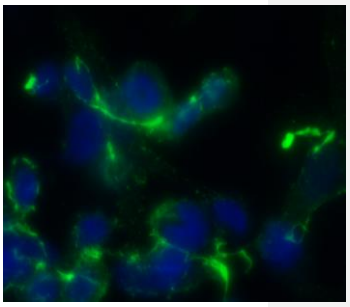

Figure 5.7: Widefield Z-stacks of location 5 in well located at column 2 row 1 in Figure 5.1. This well was treated with 180mU/mL of the enzyme heparinase III. Degradation did take place.

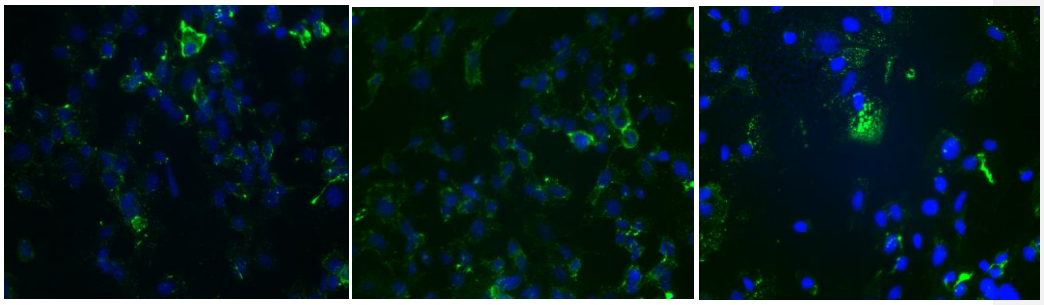

Figure 5.8: Widefield images of cells in well located in column 3 row 1 of well plate in Figure 5.1. This well was treated with 340 mU/mL of heparinase III. Locations 5-7.

Average	Maximum	Sum
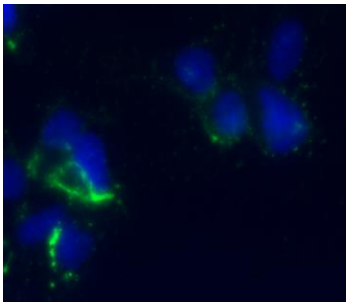	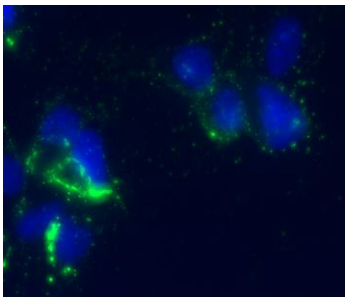	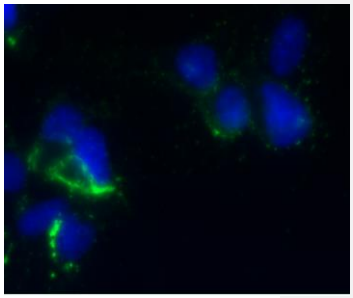

Figure 5.9: Widefield Z-stacks of cells in well located at column 3 row 1. This well was treated with 340 mU/mL of heparinase III. Location generated was location 5. Degradation did occur around the nuclei.

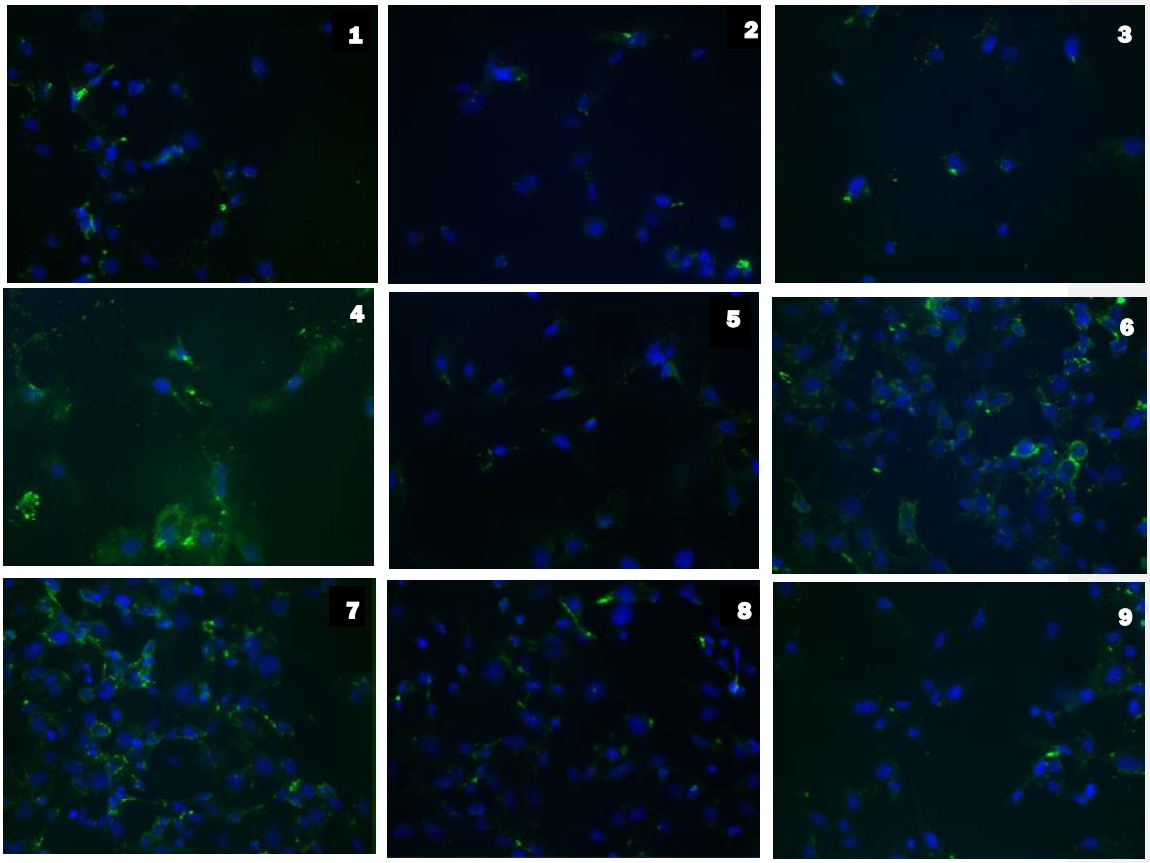

Figure 5.10: Images of well in column 4 row 1 of well plate represented in Figure 5.1. This well was treated with 500 mU/mL of heparinase III. All 9 locations were captured and represented.

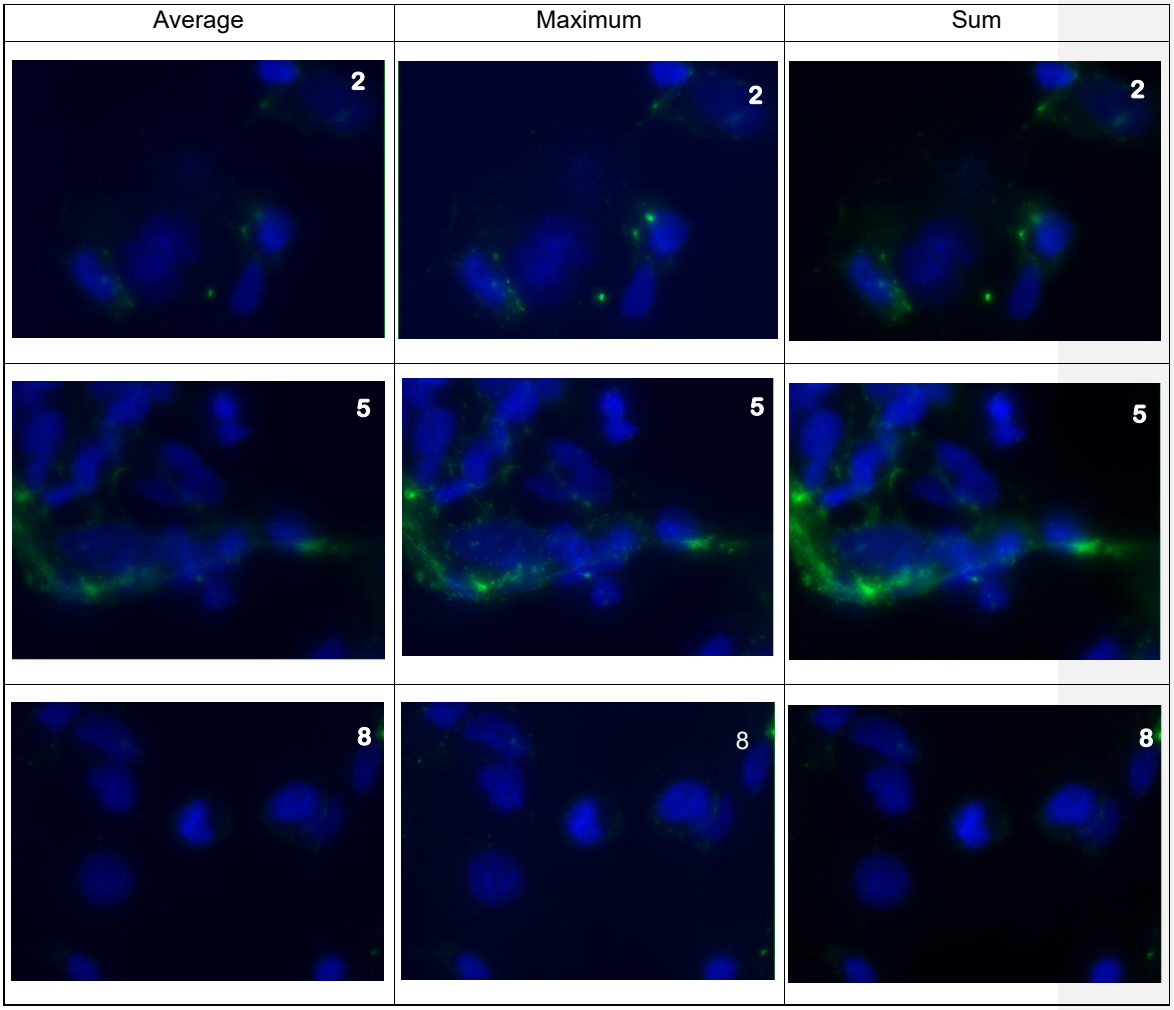

Figure 5.11: Wide field Z-stack images of well in column 4 row 1 of well plate represented in Figure 5.1. This well was treated with 500 mU/mL of heparinase III. The most degradation occurred here due to the increased enzyme concentration. Shown are selected images of locations 2, 5, 8 of the well.

Figure 5.12: Image of negative control well in Figure 5.2 column 1 row 1.

5.5 Discussion

It is apparent that the HS increasingly degrades in response to the increasing concentration of heparinase III as shown in the images depicted in Figures 5.4- 5.11. The entirety of the HS is not gone but a qualitative difference is still evident. The z-stacks shown in Figures 5.5, 5.7, 5.9 and 5.11 show a greater magnification and more accurate depiction of the degradation around each individual cell. It shows that with each increase in enzyme concentration the degradation pattern of the HS is more uniform around the cell. This could give insight as to how the HS degrades away in the body when exposed to a disturbed blood flow. The negative controls did not display a response when imaged under the microscope as intended. This lack of reaction between the secondary antibody with the HMEC-1 means that the secondary antibody is reacting exclusively with the primary antibody and is not inadvertently binding to anything else.

Figures 5.5, 5.7, 5.9 and 5.11 include z-projections of selected positions centered within the cell. These positions were chosen simply because it was likely that most of the nuclei would be present in the center of the well vs the exterior areas of the well.

All positions of the well depicted similar results in that the heparan sulfate is reduced dramatically due to the increased enzyme concentration. Figure 5.5 contains no enzyme and has heparan sulfate surrounding the entire cell as well as interconnecting between the cells implying attenuating interactions taking place. Due to these networks it has been hypothesized by other researchers that if heparan sulfate was removed to a critically low level then the entire GCX structure would collapse and stay in a diminished state [54]. It is within this well that there is a maximum coverage of heparan sulfate. Moving on to Figure 5.7 it is shown that the heparan sulfate diminished but no major significant changes occurred in comparison to Figure 5.5 . Due to previously completed research, it is assumed that at this point the thickness of the glycocalyx has started to decline [54]. Figures 5.9 and 5.11 show the greatest reduction of heparan sulfate in comparison to figure 5.5.

5.6 Conclusion

Our results support previous research on various cell lines by demonstrating that HS does degrade away in response to exponentially increasing the enzyme concentration [2, 28, 38, 53, 54]. The present study results validate the hypothesized notion that HS does lie within HMEC1 cells. In the future, a more concentrated enzyme can be utilized to see a more qualitative difference between the images.

CHAPTER 6: DISCUSSION

6.1 Overview

The GCX, and more specifically HS, has been extensively studied in multiple diseases over time. The research involved with these components and their involvement in cardiovascular disease is that of recent work, more specifically in the human species cell line. As mentioned previously chapter 2 the more common and traditional cell lines studied have been that of species bovine, pig and mouse as they are easier to obtain and work with. Though these cell lines offer great benefits to the overall goals of pathophysiology, it is important to recognize that not all cell lines respond to disease the same way. Different cell lines respond differently to different types of fluid shear stress and location of such shear stress [69]. With research being completed on this type of endothelial cell (HMEC-1) a new knowledge base is being formed on this cell line's behavior regarding CVD and other forms of stimuli. They lie within the vascular walls and are in direct contact with blood flow. Research involving these cells will give key information regarding disease progression as they play vital roles in pathological and pathophysiological processes [53].

As formerly discussed, CVD is a consequence of the inflammatory disease, atherosclerosis [5]. Inflammation builds in the arterial walls of the vascular system leading to adverse effects on the immunity of the host. Leukocytes travel to the sites of inflammation but can then start to build up. This most commonly occurs in regions of curvatures or arcs in the vasculature. The leukocyte plaque build ups can damage the arterial wall or rupture, thus consequently blood clots will form. This chain of events can

promote risk of stroke and myocardial infarction [1] [70]. With this research project, using human microvascular cells ex- vivo to study a major component of the GCX can provide a more detailed explanation of what could be occurring within the body when suffering from atherosclerosis or CVD. The GCX is a thin structure containing GAGs and sheds constantly due to its dynamic nature. Manipulating the GCX gives insight as to how shear stress can affect or completely abolish cells and the GCX's biological functions. Our current project focuses on HS within the GCX as it is the most abundant and widely studied GAG of the GCX. Overall the goals of this research were to accomplish a protocol that successfully stained the positive control and HMEC-1, observe the development of HS over time, and prove its existence through enzymatic degradation. Accomplishing these goals will help future researchers with conserving antibody if staining on the same cell line as well as reveal how HS develops over the cell over a period. These aims will be further discussed in this study.

6.2 Research Goals

Goal 1: Establish a staining protocol and confirm reliability of positive control selected

The purpose of this experiment was to confirm that the selected mouse sarcoma basement membrane heparan sulfate was positively tagging to the antibodies discussed in chapter 3. Literature review had been completed to determine an appropriate dilution ratio for the primary antibody, but the final determination was chosen in response to recommendations from Sigma Aldrich. The ratios selected (1:100 and 1:500) were tested to see if there was a significant difference between them regarding detection and image quality.

Images were obtained at random locations throughout the carefully chosen wells using a widefield confocal microscope. Results presented in figures in 3.2- 3.5 show that HS was detected and no prevalent differences between the two tested primary antibody dilutions as discussed in chapter 3. With the completion of the preliminary research discussed in chapter 3, the protocol established within the experiment can be utilized on HMEC-1 with the exact materials to detect HS.

Goal 2: Observe and image the HS development over a time of 3-7.5 days

After establishing the HS staining protocol in chapter 3, the next stage in this study was to confirm presence and development of HS on HMEC-1. The purpose of the experiment discussed in chapter 4 was to determine how long it would take HS to develop after cell culture as well as show how the development of HS progresses over a pre-determined period. Comparable research involving HS progression was conducted using human umbilical vein endothelial cells showing how the HS covered the edges of the cell before dispersing to the apical membrane over a course of two weeks.

The current research project detailed in chapter 4 followed a similar route by documenting the development over a course of 3-7.5 days post 100% confluency. It appeared that not only did the HS develop around the nucleus, but also between the cells themselves better fulfilling its role in cell-to-cell communication. The development occurred more rapidly than expected, therefore, in the future if this project were to be repeated, I would suggest that the plates be fixed and imaged every 12 hours to better document the transformation. In addition, taking images in stacks on a laser scanning microscope would be beneficial as the image quality would be clear and more precise. Another limitation with this specific study was the lack of good visualization due to the

magnification level used. The microscope most accessible for this research does not have the high-sensitive and high-resolution capabilities needed, which cannot provide finer details as desired when studying the development of the HS. Other microscopes, such as laser scanning microscopes, may be a better visualization tool for projects needing finer details or surface layer composition.

Goal 3: Verify that HS exists on the HMEC-1 by enzymatically degradation

In order to confidently confirm the existence of HS within the HMEC-1 chosen for the experiments, we must degrade away the HS. Once degraded away, using an enzyme designed to specifically target the specific component, it can be said in confidence that the HS is in fact present on the HMEC-1. The project discussed in chapter 5 covered the specifics involved in testing different enzyme dilutions and the protocol created for the enzymatic degradation process. Different dilutions of enzyme were tested for the HS on the HMEC-1. These dilutions were chosen loosely based off literature review involving numerous species as well as recommendations from the enzyme carrier tech support [2, 28, 38, 53, 54].

The amount of degradation did increase in relation to the more concentrated enzyme concentration. The HS was most degraded by the concentration of 500mU/mL of heparinase III as represented in figure 5.10 and 5.11. Figure 5.11 shows a more in detail look at the HMEC-1 up close and can provide a better visual regarding deciphering the HS degradation. It appears that the degradation does occur uniformly around the membrane. It has been shown in other research that as the HS degrades from the surface of cells, the thickness of the GCX starts to decrease as well. The thickness of the GCX is inversely related to the diffusion coefficient [37, 54]. As GAGs begin to degrade away

due to fluid shear stress and inflammation, and the thickness decreases below a specific threshold, the likelihood of the GCX collapsing increases. If the GCX collapses, the endothelial cells will then be exposed and unsupported.

6.3 Future Research

There a couple ways to proceed with this research including doing repeats on the studies already done, studying the effects of shear stress on HS development, or studying different GAGs within the GCX. It would be reasonable to go back, and repeat experiments covered in chapters 3-5 as not many samples were tested from each due to the limited amount of stock solution for reagents. This low sample size could be a limitation and testing larger sample sizes could increase the reliability of the projects. In the future it would be more dependable to have more than one repeat for each concentration of reagent being tested as done in these experiments. append

Another option to consider would be to expose the HMEC-1 to fluid shear stress by use of fluid pumps. The shear rate can be adjusted to mimic that within a blood vessel as well as exposing the cells at different stages of development. Once cells are exposed for a pre-determined amount of time, they can be fixed, stained, and imaged to see the degradation process caused by fluid shear stress. The cells can also be live-imaged while undergoing shear stress from the fluid pump by use of an incubating system built on to the microscope. This could only be possible if a non-toxic stain was acquired to use for live cell imaging. This information can be beneficial in that it could capture the possible behavior of the HMEC-1 within the vessel when exposed to disturbed blood flow.

Research involving the other main GAGs mentioned previously in chapter 2 would provide additional details in how and if the components are independent of each other. The first step could be to determine the presence of the HA and CS. This can be done using very similar protocols to that established in chapters 3-5. Once the presences of the additional GAGs are confirmed, more studies can be completed involving exposing the GAGs to fluid shear stress as mentioned previously. It would be suggested to stain all three GAGs at once thus giving insight as to if they are interconnected or their whereabouts within the cell to support previously mentioned literature [7]. Once the cells are exposed to diverse stimuli and conditions, it is possible that the sulfation patterns within the GCX can vary and modulate in response to such stimuli. Understanding how the GCX modulates over time in response to the changing biological environment can further encourage the need for research to discover a method of restoring the GCX.

CHAPTER 7: CONCLUSION

The conclusion drawn from the experiments discussed in the previous chapters is that it was proven that HS is present on the HMEC-1. This was proven by staining the HS and then enzymatically degrading it away. These results are consistent with past experiments conducted on various species and cell types. However, not all cell types respond to change within their microenvironments the same way. Human microvascular endothelial cells Type 1 that line the vasculature system can be very adaptive due to the nature of their location. This research can be very beneficial when trying to discover a solution to their more permanent degenerative behavior due to disturbed blood flow. Once the GCX ruptures, leaving the cells exposed and the production of nitric oxide ceasing, cardiovascular control starts to decline.

The literature discussed in this manuscript was utilized for recommendations on dilution factors, enzyme concentrations, and antibody selections. Additional preliminary research was conducted on HS development as represented in chapter 4. This research would need to be built on using more detailed imaging techniques and shorter time periods before fixation, staining, and imaging. Additional studies will be necessary by proving the existence of the other prominent GAGs (HA and CS) using similar methods as discussed in chapters 3-5. Once confirmed, interrelationships between the GAGs can be studied as well as their responses to different variations of fluid shear stress. Results from these recommended directions can give a better understanding as to how the HMEC-1 play a role in CVD as well as further enhance the need to make the GCX a therapeutic target.

REFERENCES

REFERENCES

1. Taleb, S., *Inflammation in atherosclerosis.* Arch Cardiovasc Dis, 2016. **109**(12): p. 708-715.

2. Ebong, E.E., et al., *Imaging the endothelial glycocalyx in vitro by rapid freezing/freeze substitution transmission electron microscopy.* Arterioscler Thromb Vasc Biol, 2011. **31**(8): p. 1908-15.

3. Mensah, S.A., et al., *Regeneration of glycocalyx by heparan sulfate and sphingosine 1-phosphate restores inter-endothelial communication.* PLoS One, 2017. **12**(10): p. e0186116.

4. Qin, Z., et al., *Extracellular superoxide dismutase (ecSOD) in vascular biology: an update on exogenous gene transfer and endogenous regulators of ecSOD.* Transl Res, 2008. **151**(2): p. 68-78.

5. Libby, P., *Inflammation and cardiovascular disease mechanisms.* Am J Clin Nutr, 2006. **83**(2): p. 456S-460S.

6. National Center for Chronic Disease Prevention and Health Promotion , D.f.H.D.a.S.P., *Heart Disease.* 2017.

7. Reitsma, S., et al., *The endothelial glycocalyx: composition, functions, and visualization.* Pflugers Arch, 2007. **454**(3): p. 345-59.

8. Cruz-Chu, E.R., et al., *Structure and response to flow of the glycocalyx layer.* Biophys J, 2014. **106**(1): p. 232-43.

9. van den Berg, B.M., et al., *Glycocalyx and endothelial (dys) function: from mice to men.* Pharmacol Rep, 2006. **58 Suppl**: p. 75-80.

10. Broekhuizen, L.N., et al., *Endothelial glycocalyx as potential diagnostic and therapeutic target in cardiovascular disease.* Curr Opin Lipidol, 2009. **20**(1): p. 57-62.

11. McDonald, K.K., et al., *Glycocalyx Degradation Induces a Proinflammatory Phenotype and Increased Leukocyte Adhesion in Cultured Endothelial Cells under Flow.* PLoS One, 2016. **11**(12): p. e0167576.

12. Florian, J.A., et al., *Heparan sulfate proteoglycan is a mechanosensor on endothelial cells.* Circ Res, 2003. **93**(10): p. e136-42.
13. Zeng, Y. and J.M. Tarbell, *The adaptive remodeling of endothelial glycocalyx in response to fluid shear stress.* PLoS One, 2014. **9**(1): p. e86249.
14. Boels, M.G., et al., *Atrasentan Reduces Albuminuria by Restoring the Glomerular Endothelial Glycocalyx Barrier in Diabetic Nephropathy.* Diabetes, 2016. **65**(8): p. 2429-39.
15. Schmidt, E.P., et al., *The pulmonary endothelial glycocalyx regulates neutrophil adhesion and lung injury during experimental sepsis.* Nat Med, 2012. **18**(8): p. 1217-23.
16. Vink, H. and B.R. Duling, *Identification of distinct luminal domains for macromolecules, erythrocytes, and leukocytes within mammalian capillaries.* Circ Res, 1996. **79**(3): p. 581-9.
17. Curry, F.R. and R.H. Adamson, *Tonic regulation of vascular permeability.* Acta Physiol (Oxf), 2013. **207**(4): p. 628-49.
18. Singh, A., et al., *High glucose causes dysfunction of the human glomerular endothelial glycocalyx.* Am J Physiol Renal Physiol, 2011. **300**(1): p. F40-8.
19. Rapraeger, A., *Transforming growth factor (type beta) promotes the addition of chondroitin sulfate chains to the cell surface proteoglycan (syndecan) of mouse mammary epithelia.* J Cell Biol, 1989. **109**(5): p. 2509-18.
20. Ushiyama, A., H. Kataoka, and T. Iijima, *Glycocalyx and its involvement in clinical pathophysiologies.* J Intensive Care, 2016. **4**(1): p. 59.
21. Watanabe, K., H. Yamada, and Y. Yamaguchi, *K-glypican: a novel GPI-anchored heparan sulfate proteoglycan that is highly expressed in developing brain and kidney.* J Cell Biol, 1995. **130**(5): p. 1207-18.
22. Kinsella, M.G., S.L. Bressler, and T.N. Wight, *The regulated synthesis of versican, decorin, and biglycan: extracellular matrix proteoglycans that influence cellular phenotype.* Crit Rev Eukaryot Gene Expr, 2004. **14**(3): p. 203-34.
23. Fu, B.M. and J.M. Tarbell, *Mechano-sensing and transduction by endothelial surface glycocalyx: composition, structure, and function.* Wiley Interdiscip Rev Syst Biol Med, 2013. **5**(3): p. 381-90.

24. Rosenberg, R.D., et al., *Heparan sulfate proteoglycans of the cardiovascular system. Specific structures emerge but how is synthesis regulated?* J Clin Invest, 1997. **100**(11 Suppl): p. S67-75.

25. Jeansson, M., et al., *Functional and molecular alterations of the glomerular barrier in long-term diabetes in mice.* Diabetologia, 2006. **49**(9): p. 2200-9.

26. Prydz, K., *Determinants of Glycosaminoglycan (GAG) Structure.* Biomolecules, 2015. **5**(3): p. 2003-22.

27. Vogl-Willis, C.A. and I.J. Edwards, *High-glucose-induced structural changes in the heparan sulfate proteoglycan, perlecan, of cultured human aortic endothelial cells.* Biochim Biophys Acta, 2004. **1672**(1): p. 36-45.

28. Jeansson, M. and B. Haraldsson, *Glomerular size and charge selectivity in the mouse after exposure to glucosaminoglycan-degrading enzymes.* J Am Soc Nephrol, 2003. **14**(7): p. 1756-65.

29. Bernfield, M., et al., *Biology of the syndecans: a family of transmembrane heparan sulfate proteoglycans.* Annu Rev Cell Biol, 1992. **8**: p. 365-93.

30. Aird, W.C., *Phenotypic heterogeneity of the endothelium: I. Structure, function, and mechanisms.* Circ Res, 2007. **100**(2): p. 158-73.

31. Tarbell, J.M. and M.Y. Pahakis, *Mechanotransduction and the glycocalyx.* J Intern Med, 2006. **259**(4): p. 339-50.

32. Pahakis, M.Y., et al., *The role of endothelial glycocalyx components in mechanotransduction of fluid shear stress.* Biochem Biophys Res Commun, 2007. **355**(1): p. 228-33.

33. van den Berg, B.M., et al., *Atherogenic region and diet diminish glycocalyx dimension and increase intima-to-media ratios at murine carotid artery bifurcation.* Am J Physiol Heart Circ Physiol, 2006. **290**(2): p. H915-20.

34. Betteridge, K.B., et al., *Sialic acids regulate microvessel permeability, revealed by novel in vivo studies of endothelial glycocalyx structure and function.* J Physiol, 2017. **595**(15): p. 5015-5035.

35. Curry, F.E. and R.H. Adamson, *Endothelial glycocalyx: permeability barrier and mechanosensor.* Ann Biomed Eng, 2012. **40**(4): p. 828-39.
36. Henry, C.B. and B.R. Duling, *TNF-alpha increases entry of macromolecules into luminal endothelial cell glycocalyx.* Am J Physiol Heart Circ Physiol, 2000. **279**(6): p. H2815-23.
37. Gao, L. and H.H. Lipowsky, *Composition of the endothelial glycocalyx and its relation to its thickness and diffusion of small solutes.* Microvasc Res, 2010. **80**(3): p. 394-401.
38. Constantinescu, A.A., H. Vink, and J.A. Spaan, *Endothelial cell glycocalyx modulates immobilization of leukocytes at the endothelial surface.* Arterioscler Thromb Vasc Biol, 2003. **23**(9): p. 1541-7.
39. Lipowsky, H.H., L. Gao, and A. Lescanic, *Shedding of the endothelial glycocalyx in arterioles, capillaries, and venules and its effect on capillary hemodynamics during inflammation.* Am J Physiol Heart Circ Physiol, 2011. **301**(6): p. H2235-45.
40. Springer, T.A., *Adhesion receptors of the immune system.* Nature, 1990. **346**(6283): p. 425-34.
41. Adamson, R.H. and G. Clough, *Plasma proteins modify the endothelial cell glycocalyx of frog mesenteric microvessels.* J Physiol, 1992. **445**: p. 473-86.
42. Tarbell, J.M. and L.M. Cancel, *The glycocalyx and its significance in human medicine.* J Intern Med, 2016. **280**(1): p. 97-113.
43. Levick, J.R., *Capillary filtration-absorption balance reconsidered in light of dynamic extravascular factors.* Exp Physiol, 1991. **76**(6): p. 825-57.
44. Merx, M.W. and C. Weber, *Sepsis and the heart.* Circulation, 2007. **116**(7): p. 793-802.
45. Lukasz, A., et al., *Endothelial glycocalyx breakdown is mediated by angiopoietin-2.* Cardiovasc Res, 2017. **113**(6): p. 671-680.
46. Ramaker, K., et al., *Absence of the Epithelial Glycocalyx As Potential Tumor Marker for the Early Detection of Colorectal Cancer.* PLoS One, 2016. **11**(12): p. e0168801.
47. Paszek, M.J., et al., *The cancer glycocalyx mechanically primes integrin-mediated growth and survival.* Nature, 2014. **511**(7509): p. 319-25.

48. Kim, Y.H., et al., *Endothelial Glycocalyx as Biomarker for Cardiovascular Diseases: Mechanistic and Clinical Implications.* Curr Heart Fail Rep, 2017. **14**(2): p. 117-126.
49. Jiang, X.Z., et al., *Large-scale molecular dynamics simulation of coupled dynamics of flow and glycocalyx: towards understanding atomic events on an endothelial cell surface.* J R Soc Interface, 2017. **14**(137).
50. Mitra, R., et al., *Glycocalyx in Atherosclerosis-Relevant Endothelium Function and as a Therapeutic Target.* Curr Atheroscler Rep, 2017. **19**(12): p. 63.
51. Bruegger, D., et al., *Atrial natriuretic peptide induces shedding of endothelial glycocalyx in coronary vascular bed of guinea pig hearts.* Am J Physiol Heart Circ Physiol, 2005. **289**(5): p. H1993-9.
52. Gouverneur, M., et al., *Fluid shear stress stimulates incorporation of hyaluronan into endothelial cell glycocalyx.* Am J Physiol Heart Circ Physiol, 2006. **290**(1): p. H458-2.
53. Bai, K. and W. Wang, *Spatio-temporal development of the endothelial glycocalyx layer and its mechanical property in vitro.* J R Soc Interface, 2012. **9**(74): p. 2290-8.
54. Zeng, Y., et al., *The structural stability of the endothelial glycocalyx after enzymatic removal of glycosaminoglycans.* PLoS One, 2012. **7**(8): p. e43168.
55. Kumagai, R., X. Lu, and G.S. Kassab, *Role of glycocalyx in flow-induced production of nitric oxide and reactive oxygen species.* Free Radic Biol Med, 2009. **47**(5): p. 600-7.
56. Salmon, A.H. and S.C. Satchell, *Endothelial glycocalyx dysfunction in disease: albuminuria and increased microvascular permeability.* J Pathol, 2012. **226**(4): p. 562-74.
57. Dominiczak, A.F. and D.F. Bohr, *Nitric oxide and its putative role in hypertension.* Hypertension, 1995. **25**(6): p. 1202-11.
58. Cheng, M.J., et al., *Endothelial glycocalyx conditions influence nanoparticle uptake for passive targeting.* Int J Nanomedicine, 2016. **11**: p. 3305-15.
59. Gromnicova, R., et al., *Transport of Gold Nanoparticles by Vascular Endothelium from Different Human Tissues.* PLoS One, 2016. **11**(8): p. e0161610.

60. Sarrazin, S., W.C. Lamanna, and J.D. Esko, *Heparan sulfate proteoglycans.* Cold Spring Harb Perspect Biol, 2011. **3**(7).
61. Torres Filho, I.P., et al., *Plasma syndecan-1 and heparan sulfate correlate with microvascular glycocalyx degradation in hemorrhaged rats after different resuscitation fluids.* Am J Physiol Heart Circ Physiol, 2016. **310**(11): p. H1468-78.
62. Biglu, M.H., M. Ghavami, and S. Biglu, *Cardiovascular diseases in the mirror of science.* J Cardiovasc Thorac Res, 2016. **8**(4): p. 158-163.
63. Sing, C.F., J.H. Stengard, and S.L. Kardia, *Genes, environment, and cardiovascular disease.* Arterioscler Thromb Vasc Biol, 2003. **23**(7): p. 1190-6.
64. Henderson-Toth, C.E., et al., *The glycocalyx is present as soon as blood flow is initiated and is required for normal vascular development.* Dev Biol, 2012. **369**(2): p. 330-9.
65. dela Paz, N.G., et al., *Heparan sulfates mediate the interaction between platelet endothelial cell adhesion molecule-1 (PECAM-1) and the Galphaq/11 subunits of heterotrimeric G proteins.* J Biol Chem, 2014. **289**(11): p. 7413-24.
66. Zeng, Y., et al., *Fluid shear stress induces the clustering of heparan sulfate via mobility of glypican-1 in lipid rafts.* Am J Physiol Heart Circ Physiol, 2013. **305**(6): p. H811-20.
67. Kang, H., et al., *Vascular smooth muscle cell glycocalyx mediates shear stress-induced contractile responses via a Rho kinase (ROCK)-myosin light chain phosphatase (MLCP) pathway.* Sci Rep, 2017. **7**: p. 42092.
68. Cooper, S., et al., *Increased MMP activity in curved geometries disrupts the endothelial cell glycocalyx creating a proinflammatory environment.* PLoS One, 2018. **13**(8): p. e0202526.
69. Reneman, R.S. and A.P. Hoeks, *Wall shear stress as measured in vivo: consequences for the design of the arterial system.* Med Biol Eng Comput, 2008. **46**(5): p. 499-507.
70. Swirski, F.K. and M. Nahrendorf, *Leukocyte behavior in atherosclerosis, myocardial infarction, and heart failure.* Science, 2013. **339**(6116): p. 161-6.

APPENDIX

Preparing Complete Growth Media

Date: April 12, 2018

Remark: (1) When 10ml of LSGS is added to 500 ml the final concentration with be Epidermal Growth Factor 10ng/ml**,** Hydrocortisone 1 μg/ml**,** Fibroblast Growth Factor 3 ng/ml**,** Heparin 10 μg/ml, and FBS 2% (v/v) (2) Therefore we will prepare the 500 ml of growth media at 8% (v/v) before adding 10 ml of LSGS.

Materials:

- Personal Protection Equipment (Nitrile gloves, lab coat, safety glasses, etc.) 500 ml bottle of MCDB131 media (No Glutamine) (#10372019, Thermo Fisher Scientific)
- Fetal Bovine Serum (FBS) (#15000044, Thermo Fisher Scientific)
- L-Glutamine (200 mM) (25030081, Gibco)
- Penicillin/Streptomycin (10,000 U/ml/10,000 μg/ml) (15-140-122, Thermo Fisher Scientific)
- Low Serum Growth Supplement (LSGS) (#S00310, Thermo Fisher Scientific)
- Serological Pipettes (one 5ml, one 10ml, two 25 ml, two 50 ml)
- Pipette Aid
- 70% Ethanol
- Kimwipes

Final concentrations in complete growth media

- FBS 10% (v/v)

- L-Glutamine 10 mM (see 'Important Notes' below)
- Penicillin/Streptomycin 100 U/ml/100 μg/ml
- Epidermal Growth Factor (EGF) 10ng/ml
- Hydrocortisone 1 μg/ml
- Fibroblast Growth Factor (FGF) 3 ng/ml

- Heparin 10 μg/ml

Method: `

- All steps are performed using aseptic techniques.
- Remove 70 ml of MCDB131 media from the bottle, leaving 430 ml of media*

- Add 40 ml of FBS (total solution volume = 470 ml)
- Add 25 ml L-Glutamine (total solution volume = 495 ml)
- Add 5 ml of Penicillin/Streptomycin (total solution volume = 500 ml)
- The total volume is 500 ml (8% v/v FBS, 10 mM L-Glutamine, 100 U/ml/100 μg/ml Penicillin/Streptomycin.
- Add 10ml of LSGS, which will increase the FBS concentration by 2% v/v. Therefore, the final concentration is ~ 10% v/v.

- * This method was selected so that the LSGS is still added to 500 ml of solution so that the final concentration of EGF, hydrocortisone, FGF, and heparin are correct.

Important Notes

1. E-mail correspondence (April 30, 2018) with ATCC regarding the recommended L-Glutamine concentration of 10mM compared to our previous protocol that used a 2mM concentration: “Thank you for your inquiry. I can confirm that the recommended glutamine concentration for CRL-3243 is 10 mM. While other vials of HMEC-1 may have been acclimated to only 2 mM of glutamine, the depositor of these cells recommended 10 mM L-glutamine. Since ATCC has not ever grown these cells using only 2 mM L-glutamine, we unfortunately do not have any information on hand about how our stocks of CRL-3243 would grow in that lower glutamine concentration. If you plan on using ATCC's stock of HMEC-1, I would have to strongly recommend switching to the higher concentration glutamine.

2. The FBS concentration of the LSGS is 95%. If we add the LSGS to 500ml, the final concentration, Cf, is Ci Vi = Cf Vf, 95% (10ml) = Cf 500ml, Cf = 95% (10/510) = 1.86% ~ 2%

3. Confirmed with Thermo Fisher technical help (by phone, March 21, 2018) that the LSGS is compatible with MCDB131 media

Handling Procedure for Frozen Cells (From ATCC)

Date: May 2, 2018

Remark:

(1) Adapted from the recommended protocol from the American Type Culture Collection (ATCC), and e-mail correspondence with ATCC.

(2) **Important**: It is suggested that, prior to the addition of the recovered cells, the culture vessel(s) containing the complete growth medium that will be used to culture/incubate the cells be placed into the incubator for at least 15 minutes to allow the complete growth media to reach its normal pH (7.0 to 7.6).

(3) **Important:** When aspirating liquid from culture vessel work quickly/smoothly so that the time the cells are not covered with liquid is minimal.

Materials:

- Personal Protection Equipment (Nitrile gloves, lab coat, safety glasses, etc.)
- Biosafety Cabinet (BSC) – set up properly and sterilized
- Water bath, 37°C (only use bath next to CO_2 incubator)
- Prepared complete growth media for HMEC-1 (see protocol)
- Serological pipettes
- Pipette Aid

- Sterile 15-ml conical tubes
- Sterile culture vessel(s) (e.g., T-75 flask)
- 70% Ethanol
- Kimwipes

Method: `

- Pre-warm complete growth medium to 37°C before use. Minimize dwell time. Spray complete growth medium bottle with 70% Ethanol and wipe with a Kimwipe. Transfer to BSC.
- Thaw the vial by gentle agitation in a 37°C water bath. To reduce the possibility of contamination, keep the O-ring and cap out of the water. Thawing should be rapid (~ 1-2 minutes).

- Remove the vial from the water bath as soon as the contents are thawed, then decontaminate by spraying with 70% ethanol and wipe with a Kimwipe.
- Transfer the vial to the BSC. All of the operations from this point on should be carried out under strict aseptic conditions.
- Transfer the vial contents to a 15-ml centrifuge tube then slow add 9.0 mL complete culture medium and centrifuge at 275 x *g* for 10 minutes.
- After centrifugation, remove supernatant (this step removes the DMSO) and resuspend cell pellet with recommended complete medium (see the specific batch information for the culture recommended dilution ratio). Note: the cell concentration (cells/ml) should be available either from ATCC (if vial was purchased from ATCC), or when the cells were frozen in house.
- Transfer contents at the appropriate seeding density to the culture vessels (e.g., T-75 flask). It is important to avoid excessive alkalinity of the medium during recovery of the cells. It is suggested that, prior to the addition of the recovered cells, the culture vessel(s) containing the complete growth medium be placed into the incubator for at least 15 minutes to allow the medium to reach its normal pH (7.0 to 7.6). Note: see subculturing protocol for recommend working volume for culture vessels.

- Incubate the culture at 37°C, 5% CO2 in air atmosphere.
- Examine the culture after 24 hours.
- Then, check the culture every day to see if it needs media. Normally, media will be replaced every 2-3 days.

Important Notes

1. 275 x g for 10 minutes recommended by ATCC (e-mail correspondence, May 7, 2018)

2. If you notice you pellet tends to dislodge from the centrifuge tube before you can aspirate the supernatant, you may wish to increase the spin down speed.

3. For the incubation of the complete growth media in the incubator, it refers to only the media that the cells will be placed in for incubation/culture. The media that is used to dilute the cells after thawing prior to the spin down to remove the DMSO does not need to be incubated in the incubator prior to use. The final media the cells will be in to incubate should be incubated for 15 minutes prior to use to help equilibrate in the incubator.

Positive Control Heparan Sulfate Staining Protocol:

H4777, 10E4 epitope, AF 488, IBIDI 24 Well Plate

Date: April 8, 2019

Remarks

1. Experiment includes H4777 Heparan Sulfate, 10E4 epitope primary antibody, ABCAM 488 secondary antibody and IBIDI 24 well plates
2. Positive Control H4777 must be aliquoted previously in intended concentrations
3. Primary and Secondary Antibodies should be prepared right before use
4. Working volume = 0.5 – 1 mL; 350 uL just to cover bottom of well

Materials:

- Heparan Sulfate Proteoglycan (H4777 Sigma Aldrich)
- Primary Antibody H1890 Mouse Anti-Heparan Sulfate 10E4 epitope (H1890, US Biological Life Sciences)
- Secondary Antibody Goat anti-mouse Alexa Fluor 488 (ab150113 ABCAM)
- 1% (w/v) Bovine Serum Albumin (BSA) (Sigma Life Science)
- PBS Buffer, (#20012-043, Thermo Fisher Scientific)
- DPBS (#14190-144, Gibco)
- Centrifuge
- CO_2 Incubator
- IBIDI 24 Well Plate (#82406, Ibidi)
- IBIDI Mounting Medium (#50001, Ibidi)
- Fibronectin (#33016-015 , Thermo Fisher Scientific)
- Kim Wipes
- Heparan Sulfate (#H4777, Sigma Aldrich)
- Micropipette (#53510-037, Thermo Fisher Scientific)
- Pipette

Prepare Solutions:

- Day 2: Solution A: 1% BSA in PBS
- Day 2: Primary Antibody Solution (1:100) (1:500) in BSA (Solution A)
- Day following Primary Antibody – Secondary Antibody (1:500) mixed in Solution A

  IMPORTANT this solution must be protected from light
  - Spin down mixed antibody solution at _ x g for 5 minutes
- Day 1: Fibronectin aliquot of 240 ug/mL mixed with 12 mL DPBS to get 20ug/mL

Method:

Day 1 :

1. Add 400 uL of Fibronectin (20 µg/ml) to each well
2. Incubate plate in CO_2 Incubator for at least 1 hour
3. Remove fibronectin solution
4. Add 350 uL of Positive Control H4777 (concentrations 0.5, 0.75, 1 ug/mL) to intended wells
5. Insert plate into Ziploc bag with a wet Kim-wipe and store in 4°C (fridge) overnight

Day 2:

6. Aspirate excessive Positive Control
7. Add 300 uL of Primary Antibody to intended wells
8. Place plate in humidified chamber with wet Kimwipe and incubate at 4°C (fridge) overnight

Day 3:

9.
10. Aspirate excessive primary antibody and wash with 350 uL of Solution A (3 x 2 minutes)
    ** AS NEEDED: After each wash pat dry with Kim-wipe
    Do so by twisting wipe to a fine point and putting it in the bottom corner of the well to soak up excess liquids
11. Apply Secondary Antibody AF 488 (1:500) (350 uL/well)

    ** After this step always protect samples from light

12. Place well plate in Ziploc bag with wet Kim-wipe and place in light box wrapped with aluminum foil
13. Incubate in the dark for 2 hours at room temperature
14. Aspirate Secondary Antibody AF 488 from each well and wash 5 x 2 minutes with 400 uL/well of Solution A
    ** AS NEEDED: After each wash pat dry with Kim-wipe as described previously in step
15. Samples are ready for ProLong drops and imaging
    **Imaging can occur immediately following mounting or stored at 4 degrees C (dark protected from light)

Commented [KR3]: Don't know if this much fibronectin is necessary

Commented [LD4]: What concentration?

Commented [LD5]: Concentration?

Commented [LD6]: or use ProLong and coverslip

Preparation of 4% (w/v) Paraformaldehyde in PBS

Date: February 23, 2018

Materials:

- Personal Protection Equipment (Nitrile gloves, lab coat, safety glasses, etc.)
- Chemical fume hood
- Stir/heat plate, with magnetic bar (Note: this will need to chemical fume hood)
- Analytical Balance (glass encased) (Note: this will need to chemical fume hood)
- Glass beaker (volume depends on volume of 4% Paraformaldehyde preparing
- Paraformaldehyde (PFA) (#158127, Sigma-Aldrich)
- 1X Phosphate buffered saline (PBS) (#20012043, Thermo Fisher Scientific)
- NaOH (10M, #72068, Sigma-Aldrich)
- HCL (#H1758, Sigma-Aldrich)
- pH strips
- Serological pipettes (volumes depend on quantity of 4% PFA preparing)
- Pipette Aid
- Weigh boat
- Transfer pipettes (one for NaOH, one for HCL)
- 0.45µm syringe filter
- Aluminum foil

Method:

- Place analytical balance and stir/heat plate in a chemical fume hood. Notes: (1) all work preparing 4% PFA must be performed in a fume hood. Aluminum foil should be placed in fume hood work area to help with clean up. (2) place aluminum foil on stir/heat plate.
- EXAMPLE: To prepare 1 L of 4% (w/v) Formaldehyde, add 800 mL of 1X PBS to a glass beaker on a stir/heat plate in a chemical fume hood. Heat while stirring to approximately 60°C. Do not heat above 60°C. Note: This is an example, adjust volume according to final desired volume (e.g., add approximately ~ 80% of final volume).

- EXAMPLE: Add 40 g of paraformaldehyde powder to the heated PBS solution. Note: This is just an example, adjust according to final desired volume.
- The powder will not immediately dissolve into solution. Slowly raise the pH by adding 1 M NaOH dropwise from a pipette until the solution clears. Note: be patient – add drops slowly.
- Once the paraformaldehyde is dissolved, the solution should be cooled to room temperature and filtered with a 0.45µm syringe filter.
- Adjust the volume of the solution to 1 L with 1X PBS. Note: This is just an example, adjust according to final desired volume.
- Re-check the pH of the solution and adjust it with small amounts (dropwise) of dilute HCl to approximately 7.2**.** Note: Add only 1 drop, then check pH.

- Although best prepared fresh for each experiment, 4% (w/v) Paraformaldehyde can be stored for ~ 1-2 weeks at 4°C protected from light.

Staining of HMEC1 and Heparan Sulfate in µ-slide 8 Wells

Date: May 9, 2019

Remarks

5. Experiment includes 10E4 epitope primary antibody, ABCAM 488 secondary antibody and IBIDI µ-slide 8 well
6. Positive Control H4777 must be aliquoted previously in intended concentrations (if aliquots are big enough)
7. Must follow "Handling Procedure for Frozen Cells" prior to this protocol
8. Primary and Secondary Antibodies should be prepared right before use
9. Working volume = 0.3 mL; 150-180 uL just to cover bottom of well
10. Check cultures every day for contamination and to exchange media

Materials:

- Primary Antibody H1890 Mouse Anti-Heparan Sulfate 10E4 epitope (H1890, US Biological Life Sciences)
- Secondary Antibody Goat anti-mouse Alexa Fluor 488 (ab150113 ABCAM)
- 1% (w/v) Bovine Serum Albumin (BSA) (Sigma Life Science)
- PBS Buffer (#20012-043, Thermo Fisher Scientific)
- Hoechst
- Formaldehyde (#158127-100, Sigma Aldrich)
- Goat Serum (#G9023, Sigma Aldrich)
- Glycine
- Aluminum Foil
- Refrigerator
- Centrifuge
- CO_2 Incubator
- IBIDI µ-slide 8 Well Plate (#80826, Ibidi)
- IBIDI Mounting Medium (#50001, Ibidi)
- Kimwipes
- Micropipette (##53510-037, Thermo Fisher Scientific)
- Pipette (#, Thermo Fisher Scientific)
- Human microvascular endothelial cells type 1

Prepare Solutions:

- Day 1: Solution A: 0.1% BSA in PBS (wash buffer)
- Day 1: Solution B (Blocking Buffer): Goat Serum (1:10) & 0.3M Glycine in Solution A
- Day 1: Solution C : 4% PFA in PBS
- Day 1: Primary Antibody Solution (noted concentrations in lab book) in Solution A
- Day following Primary Antibody (Day 2) – Secondary Antibody (1:500) in Solution A

Commented [RK7]: Add this information

IMPORTANT this solution must be protected from light

- Spin down mixed antibody solution at _ x g for 5 minutes

o Hoechst (1:1000) 1x stock solution in Solution A

Method:

Day 1:

16. Remove HMEC1 well plate from incubator
17. Wash cells twice with prewarmed PBS (300uL/well)
18. Fix cells in solution C for 10 minutes at room temperature (150 uL/well)
19. Wash with solution A (3 x 5 minutes) (300uL/well)
20. Block with Solution B for 30 minutes at room temperature (150 µL/well)
21. Aspirate blocking solution and blot thoroughly on HMEC1 plate
22. Add 150 uL of Primary Antibody to intended wells of HMEC1 plate
23. Place plate in humidified chamber with wet Kimwipe and incubate at 4°C (fridge) overnight

Day 2:

24. Aspirate excessive primary antibody and wash with 300 uL of Sln A (3 x 2 minutes)
    ** AS NEEDED: After each wash pat dry with Kim-wipe
    Do so by twisting wipe to a fine point and putting it in the bottom corner of the well to soak up excess liquids
25. Apply Secondary Antibody AF 488 (1:500) (150 uL/well)

    ** After this step always protect samples from light

26. Place well plates in Ziploc bag with wet Kim-wipe and place in light box wrapped with aluminum foil
27. Incubate in the dark for 2 hours at room temperature
28. Aspirate Secondary Antibody AF 488 from each well and wash 5 x 2 minutes 300 uL/well with Sln A
    ** AS NEEDED: After each wash pat dry with Kim-wipe as described previously in step
29. Apply Hoechst (1:1000) for 5 minutes at room temperature (150µL)
30. Wash with PBS (3x10 minutes) (300 µL)
31. Samples are ready for IBIDI mounting drops and imaging
    **Imaging can occur immediately following mounting or stored at 4°C (in dark protected from light)

Enzyme Degradation of Heparan Sulfate on HMEC-1 Protocol

Remarks

- Heparinase III powder reconstituted into master stock
- (X) days after desired confluence is reached, cells are ready for enzymatic degradation
- Protocol needs to be followed in culture hood
- Will need to refer to “Handling Procedure for Frozen Cells” Protocol prior to this protocol
- Will need to refer to “Positive Control Heparan Sulfate” Protocol steps 1-6 prior to this protocol

Materials

- Serum free media
- IBIDI µ-slide 8 Well Plate (80826, IBIDI)
- Micropipette (##53510-037, Thermo Fisher Scientific)
- Human microvascular endothelial cells type 1
- Formaldehyde (product number,__)
- CO_2 Incubator
- Heparinase III (H8991, Sigma Aldrich)

Method

1. Reconstitute heparinase III from master stock by diluting in serum free media (180mU/mL, 340 mU/mL, 500 mU/mL)
2. Apply heparinase III to intended wells (150µL/well)
3. Incubate HMEC1 with heparinase III for 2 hours in incubator
    - Control plate can be set out at room temperature with heparinase III
4. Aspirate heparinase from intended wells
5. Wash with prewarmed PBS (3x5 minutes) (300uL)
6. Immediately following completion of enzymatic degradation, fix HMEC1 with 4% PFA for 10 minutes at room temperature
    - Follow staining of HMEC1 protocol
    - Follow Positive Control Heparan Sulfate